# 11

Functional Nanomaterials using the Cu-catalyzed Huisgen Cycloaddition Reaction

Sander S. van Berkel, Arnold W.G. Nijhuis, Dennis W.P.M. Löwik and Jan C.M. van Hest

11.1   Introduction

Nanomaterials represent various materials with the resembling property that their size is 'nano' in at least one dimension. The definition of 'nano' is somewhat arbitrary, but in the majority its magnitude is considered to vary from approximately 10 to 100 nm. Nanomaterials are utilized in many applications. Colloidal gold (gold nanoparticles in suspension), for instance, can be used to stain glass with an intense red color as was done in ancient times. Recent examples are zinc nanoparticles in sun block creams and cancer medicine delivered by liposomes. For the future, countless applications of nanoparticles are anticipated. For these applications nanomaterials need to be connected to the macroscopic world via their exterior. Hence, the modification of nanomaterials to acquire the desired exterior functionality is of major importance to utilize nanomaterials effectively in practical applications.[1] Modification of nanomaterials to obtain specific functionality is often only feasible when highly selective and efficient reactions are used. Sharpless classified reactions that meet such challenges as click reactions.[2] In respect of click chemistry the Cu-catalyzed Huisgen 1,3-dipolar cycloaddition of azides and terminal alkynes has received a lot of attention.[3,4] This cycloaddition unites azides and alkynes regio-specifically to yield 1,4−disubstituted 1,2,3-triazoles. In this review the functionalization of nanosized materials via this conjugation method is described going from inorganics such as silicon, CdSe, magnetic and gold nanoparticles, to carbon-based materials such as fullerenes and carbon nanotubes. Moreover
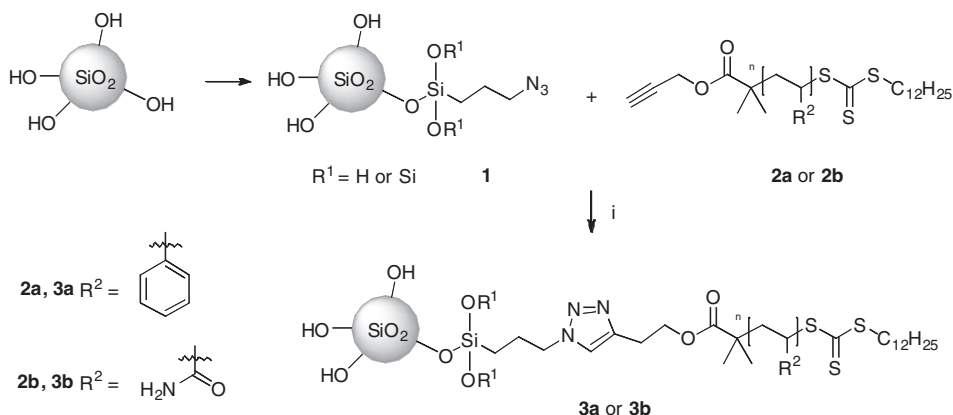
Scheme 11.1   *Grafting of acetylene polymers prepared via RAFT to nanoparticle **1**. Reaction conditions: (i) CuSO4–sodium ascorbate; DMSO; 50°C.[8]*

organic and bio-organic, self-assembled systems will be discussed, viz. polymeric micelles, polymersomes, liposomes and virus particles that have also been employed as a scaffold in the Cu-catalyzed azide alkyne cycloaddition.

11.2   Inorganic Nanoparticles

When inorganic materials are downsized to nanometer dimensions new properties, found neither in bulk nor in molecular systems, arise. For example the electronic, optical and magnetic properties of metal and semiconducting nanoparticles strongly depend on their size and shape.[5] Moreover, surface functionality is an important aspect of such nanoparticles due to the relatively large surface-to-volume ratio. In this section click chemistry employed to functionalize silicon, CdSe, magnetic and gold nanoparticle surfaces is surveyed.

11.2.1   Silicon-based Nanoparticles

Modified organic colloidal silica is of particular interest due to the ease of synthesis of well-defined particles and finds applications in stationary chromatography phases, coatings and sensors.[6,7] To render silica nanoparticles compatible with polymer systems Brittain and coworkers have modified silica nanoparticles with azides and attached a variety of acetylene functionalized macromolecules.[8] 3-Bromopropyltrichlorosilane was deposited on colloidal silica, with dimensions of 75–100 nm. Under Schlenk conditions, the bromides were exchanged for azides to obtain azide–silica-particle **1** as shown in Scheme 11.1. Acetylene functional polystyrene (PS) **2a** and polyacrylamide (PAAm) **2b** were synthesized via a reversible addition fragmentation technique (RAFT) with acetylene functional initiators. Employing CuSO4–ascorbic acid-catalyzed click reactions, these polymers were grafted to yield silica nanoparticles **3a** and **3b**.

Complementary to this 'grafting-to' approach, polymers were also 'grafted from' nanoparticle **1**.[9] A RAFT initiator was clicked onto nanoparticle **1** and subsequently polymerization was initiated. 'Grafting-from' has the advantage that low molecular weight monomers diffuse to the surface, while 'grafting to' concerns the mobility of high molecular weight polymers. For that reason the grafting density is generally higher when the 'grafting from' approach is applied. With elemental analysis grafting densities of 0.29 groups nm^{-2} were found for the 'grafting to' approach whereas 0.68 groups nm^{-2} were found for 'grafting from'. Interestingly, when the cycloaddition reaction and polymerization were performed simultaneously in a tandem process an intermediate grafting density was obtained.[10] CuBr–N,N,N',N'',N''-pentamethyldiethylenetriamine (PMDETA) was used as catalyst in this tandem process because it proved to be compatible with the RAFT polymerization. Using 0.01 mol% catalyst a grafting density of 0.51 groups nm^{-2} according to elemental analysis was found. When 0.1 mol% copper catalyst was used a grafting density of 0.70 groups nm^{-2} was observed. With this large quantity of catalyst available the click reaction was faster and thus shorter RAFT polymers were clicked to nanoparticle **1** from where the polymerization continued. Using more catalyst in the tandem process thus made it resemble more the 'grafting-from' approach.

11.2.2 Cadmium Selenide-based Nanoparticles

Semiconducting nanoparticles such as CdSe are also known as quantum dots and have attracted widespread research interest because of their tuneable optical properties and potential applications in the field of biomedical imaging, photovoltaic cells and nano-electronics.[1,11] Alkane phosphinoxide-ligands used to stabilize CdSe nanoparticles can be replaced with azide-modified phosphinoxide-ligands via ligand-desorption using pyridine and subsequent ligand exchange (Scheme 11.2).[12] In the same way alkane phosphinoxide ligands were replaced with acetylene phosphinoxide ligands.[13] Employing either CuBr–tris-(benzyltriazolylmethyl)amine (TBTA) catalysis or purely thermal conditions (95 °C) for the Huisgen cycloaddition reactions a variety of molecules, depicted in Scheme 11.2, bearing acetylene or azide groups were attached to nanoparticles **5** and **6** respectively.[12,13] Applying heat led to an inseparable mixture of 1,4- and 1,5-regioisomers as expected while the Cu catalyzed reactions provided exclusively 1,4-regioisomer in quantitative yields. To check if substrates were really covalently attached to the nanoparticles, nanoparticle **7c** was used. Nanoparticle **7c** contains barbituric acid which can bind to the Hamilton bisaminopyridine receptor as shown in Figure 11.1(c). Self-assembled monolayers on gold wafers containing the Hamilton receptor were treated with the barbituric acid nanoparticles **7c**. As a control experiment nonfunctional nanoparticles **4** were used. AFM measurements showed a dense layer of nanoparticles covering the gold wafer in the case where the nanoparticles **7c** were used [Figure 11.1(a)]. Relatively little nonspecifically bound particles were present in the control experiment [Figure 11.1(b)].

11.2.3 Ferric Oxide-based Nanoparticles

Magnetic iron oxide nanoparticles with the appropriate surface modifications can be used in a variety of applications. Examples of the use of magnetic nanoparticles (MNP) include magnetic resonance imaging contrast agents, biosensing, drug-delivery and hyperthermia.[14] Oleic acid ligands, coating magnetic nanoparticles, can be replaced with
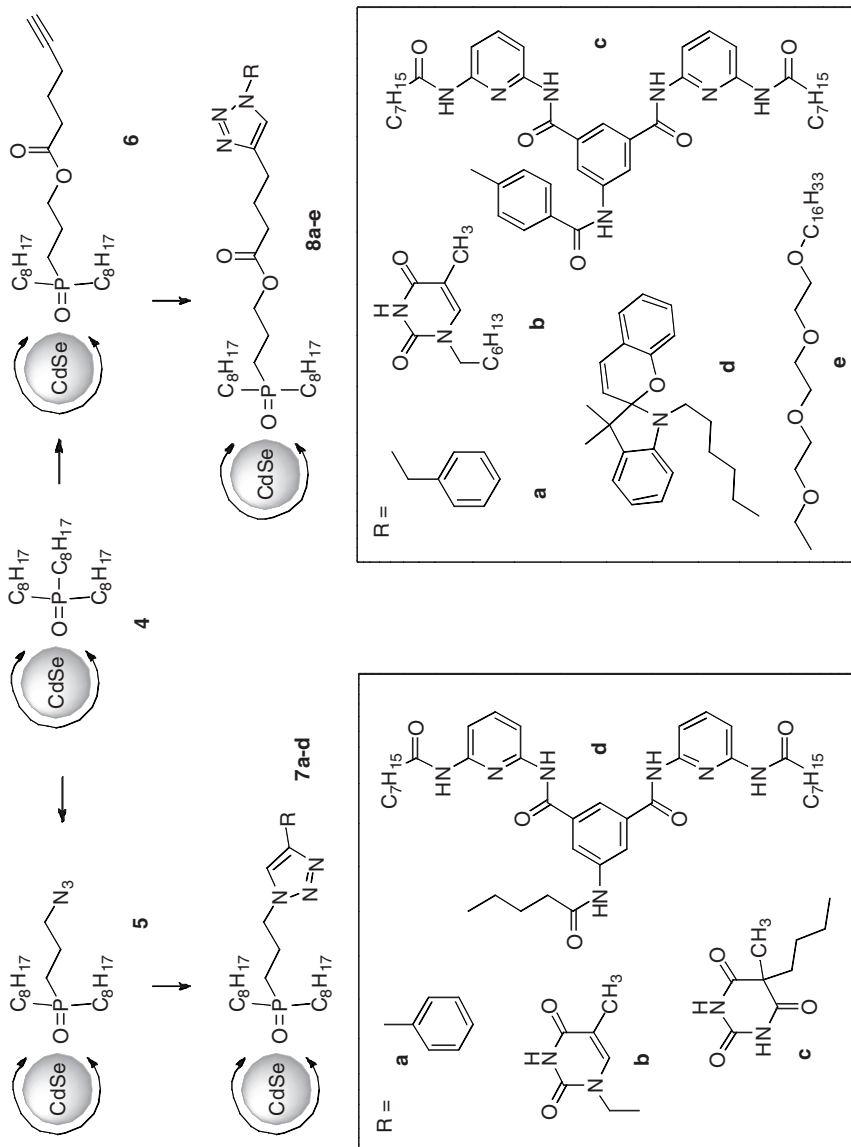
Scheme 11.2 *Replacement of phosphinoxide-ligands with azide or acetylene derivatives, and click reactions of functional molecules with nanoparticles **5** and **6**.*[12,13]
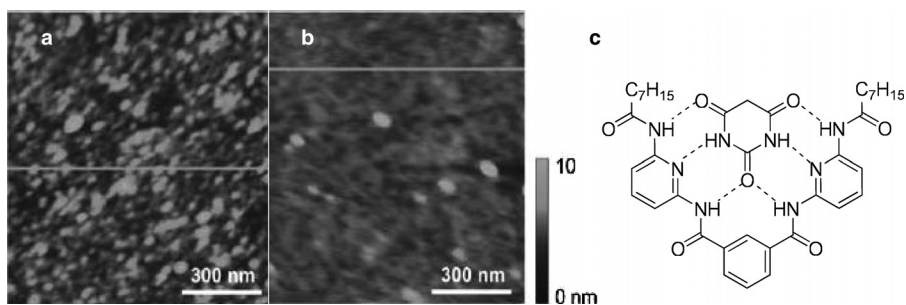
Figure 11.1 *Gold surface containing the Hamilton receptor treated with nanoparticles **7d** (a) and **4** (b). Interaction between barbituric acid and the Hamilton receptor (c). Reprinted with permission from ref.[13]. Copyright 2007 Royal Society of Chemistry.*

acetylene (**9**) or azide (**10**) containing ligands, providing functionality for further modification (Scheme 11.3).[15]

MNP **9** was attached to benzyl azide and MNP **10** to chloropentyne via the click reaction, using CuSO$_4$–sodium ascorbate as catalyst. After recovering the particles via extraction with organic solvents FTIR showed loss of azide respectively acetylene and appearance of triazole absorbance bands, indicating that the click reaction had proceeded. α-Acetylene-poly(*tert*-butyl acrylate) acid was clicked with MNP **10** under similar conditions to demonstrate that complex functionalities could be introduced. Again the FTIR spectrum showed disappearance of the azide peak.

Another application of these MNPs was explored by Gao and coworkers who investigated the possibility of recycling Pd catalysts.[16] They coated MNPs with a layer of silica and subsequently attached an azide functionalized silane to obtain MNP **11** (Scheme 11.4). Attachment of acetylene dipyridyl to MNP **11** was performed via a CuI-catalyzed click reaction. The corresponding Pd–dipyridyl complex was formed by refluxing the dipyridyl MNP together with PdCl$_2$(MeCN)$_2$ in toluene. MNP **12** was then used to catalyze Suzuki coupling reactions between aryl halides and aryl boronic acid. MNP **12** was easily removed
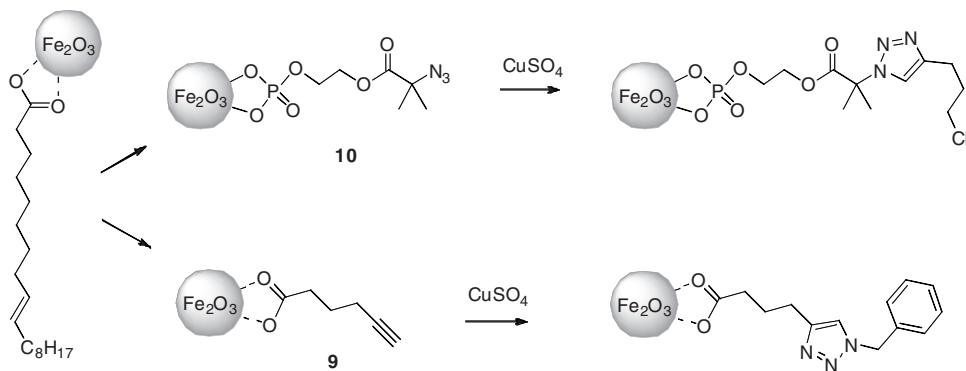
Scheme 11.3 *Replacement of oleic acid from Fe$_2$O$_3$ with azide or acetylene functionalized ligands.[15]*
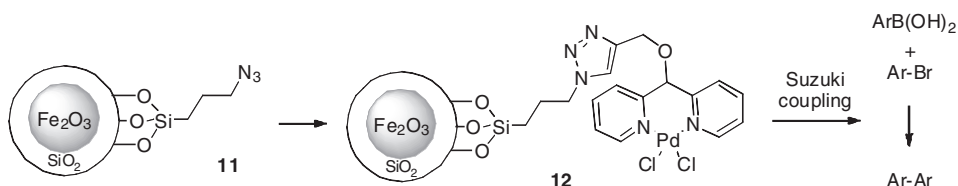
Scheme 11.4 *Functionalization of MNP with Pd catalyst. Reaction conditions for the click reaction: CuI; DIPEA; DMF–THF (1:1).[16]*

afterwards by applying an external magnetic field and it was shown that after several consecutive runs the complex retained activity.

Von Maltzahn *et al.* attached the so-called Lyp-1 targeting peptide to MNPs for precisely targeting biological locations.[17] LyP-1 binds to p32 mitochondrial proteins that are overexpressed in human cancers. The peptide sequence CGNKRTRGC was modified with an acetylene and a fluorophore as shown in Figure 11.2(a). Azido functional MNPs were coated with peptide **13** via copper-catalyzed Huisgen cycloaddition. The obtained MNP-**13** conjugates [Figure 11.2(b)] were stable *in vivo* for more than 5 h and were shown to accumulate in MDA-MB-435 cancer cells, see Figure 11.2(c), whereas control azido-bearing particles did not.

Several acetylene functional proteins, i.e. enhanced green fluorescent protein (EGFP),[18] maltose binding protein (MBP)[18] and human serum albumin (HSA),[19] were clicked to azide functional magnetic nanoparticles. Acetylene–EGFP and MBP were prepared via the expressed protein ligation method.[20] HSA was modified with an alkyne at the only
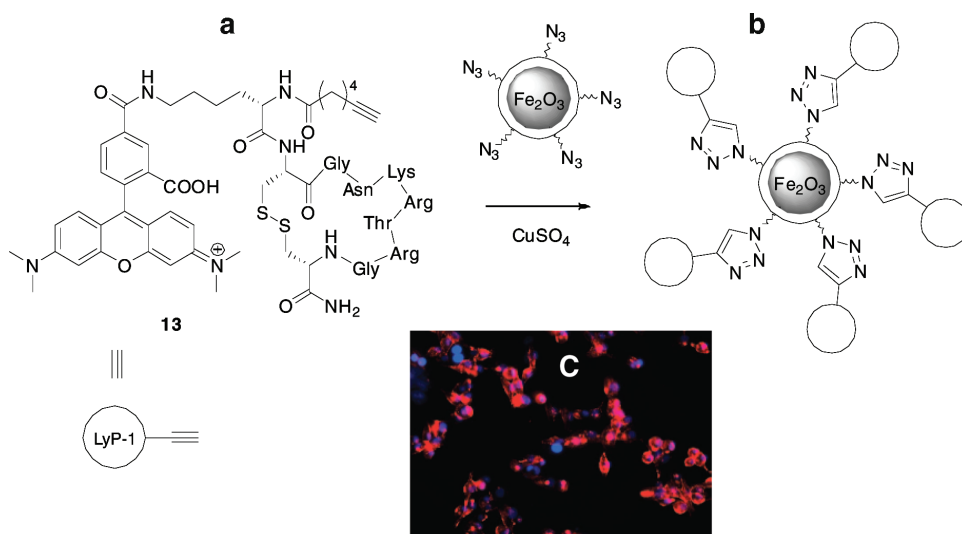

Figure 11.2 *(a) Modified LyP-1 targeting peptide. (b) MNP–**13** conjugate. (c) Fluorescence imaging of MDA-MB-435 cancer cells incubated with MNP–**13** conjugate (red), nuclear stain cells (blue). Reprinted with permission from ref.[17]. Copyright 2008 American Chemical Society.*
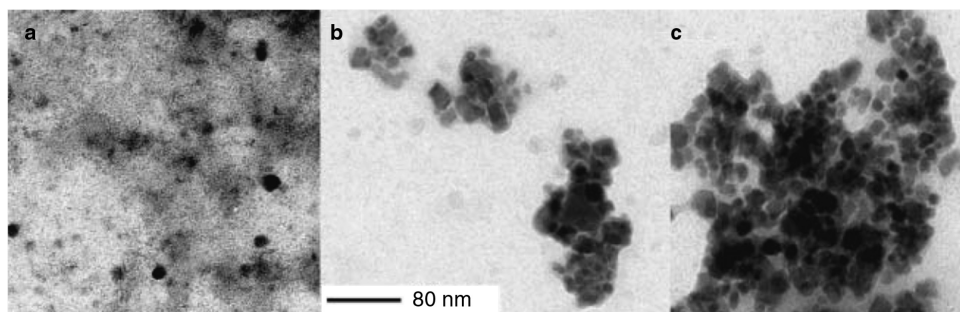
Figure 11.3 *TEM images of different stages of HSA-MNP agglomeration in response to addition of anti-HSA: (a) 0.02 mg ml⁻¹ HSA-MNP in 0.1 M phosphate buffer (pH 7.0); (b) same as (a) with addition of 0.01 mg ml⁻¹ anti-HSA; (c) same as A with addition of 0.10 mg ml⁻¹ anti-HSA. Reprinted with permission from ref.[19]. Copyright 2008 Royal Society of Chemistry.*

cysteine residue present, via Michael addition of an alkyne-bearing acrylamide. EGFP with an acetylene attached to its C terminus was clicked with azido MNPs similar to particles **11** employing the Huisgen cycloaddition. Covalently bonded to the MNP, EGFP was shown to exhibit the expected fluorescence signal at 530 nm. MBP was attached to MNP in two different ways, site-specifically at its C terminus via the click reaction or randomly via amide bond formation with lysine and arginine residues. Both MBP-MNPs were incubated with biotinylated maltose and the bound maltose was visualized with fluorescently labeled streptavidin-Cy3. The fluorescence intensity of the site specifically attached MBP-MNP was approximately twice as high as the intensity of the MBP-MNP attached via random amide bond formation. The decreased fluorescence was explained by the fact that the random attachment can cause blocking of the binding site. Finally HSA-MNP conjugates were prepared via the click reaction. Solutions of HSA-MNP were incubated with different amounts of anti-HSA polyclonal antibody (which can bind two HSA units). The level of agglomeration of the HSA-MNP corresponded nicely to the amount of antibody added, as is shown in Figure 11.3.

11.2.4 Gold-based Nanoparticles

Gold nanoparticles possess chemically and physically interesting properties that potentially makes them employable in the field of medical diagnostics, catalysis and imaging.[21] To prevent gold nanoparticles from aggregating they are usually stabilized with alkanethiol ligands. To add functionality to gold nanoparticles the alkanethiol ligands can be replaced with functional ligands in an exchange process, yielding particles with diverse properties such as high water solubility and fluorescence. A drawback is the need to synthesize the individual thiol ligands separately. Therefore post-exchange modification is often performed instead, using a variety of reactions such as nucleophilic substitution, amide bond formation and olefin metathesis. Cycloaddition click chemistry is utilized in this respect as a complementary method to introduce new functionalities to gold nanoparticles under mild and orthogonal conditions. To modify gold nanoparticles via the CuAAC reaction, azides or alkynes have to be present at the nanoparticle surface. In Scheme 11.5 a variety of alkyne
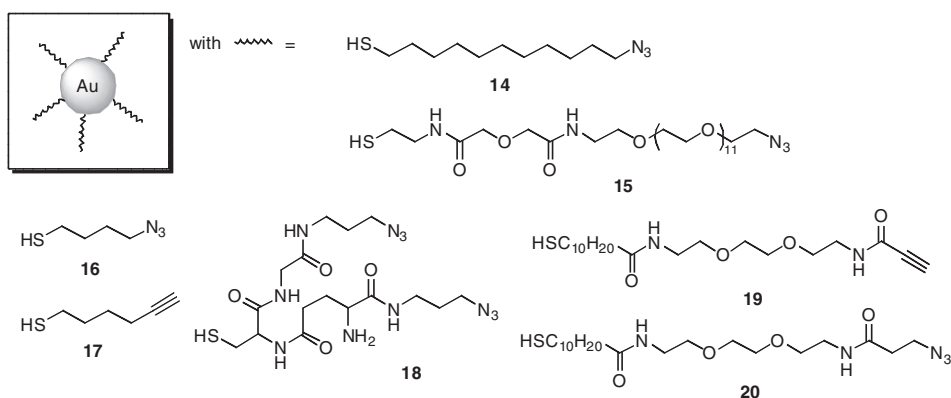
Scheme 11.5   *Examples of clickable gold nanoparticles (**14**,[22–25] **15**,[26] **16**,[27] **17**,[27] **18**,[28] **19**,[29] **20**[29]).*
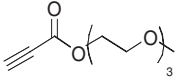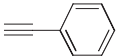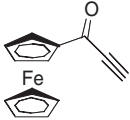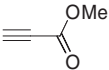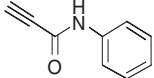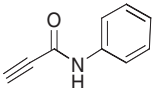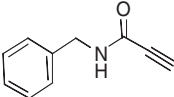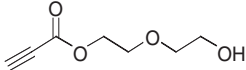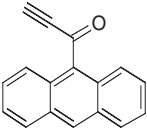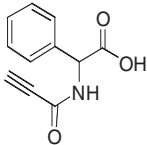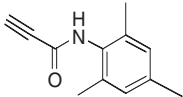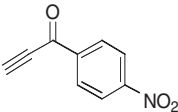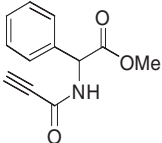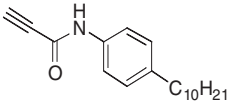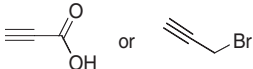
and azide functional ligands are depicted, which have been used to replace alkane thiol ligands and hence introduce the desired functionality.

Williams and coworkers partially exchanged decanethiol ligands on gold nanoparticles with azide-functionalized ligands to obtain azide-functionalized gold nanoparticles **14** soluble in organic solvents.[23] These nanoparticles precipitate from solutions containing polar solvents, i.e. THF–H_2O, DCM–EtOH and dioxane. Because of the hydrophobicity of the particles, only click catalysts soluble in organic solvents were explored, including CuI, (PPh3)3-CuBr and CuBr–2,6-lutidine. Nevertheless, all catalysts tested were found to cause extensive particle aggregation. Others who used identical gold nanoparticles also observed this aggregation phenomenon.[25] Therefore, cycloaddition reactions were performed in the absence of a catalyst. To provide a more electron-withdrawing environment, which is known to enhance the rate of triazole formation, a series of electron poor acetylene containing molecules was used (Table 11.1).

Williams and coworkers reported conversions of azides to triazoles typically ranging from 5 to 15% after 60 h reaction time. Yields improved when dioxane–hexane 1:1 instead of neat dioxane was used as solvent. From varying the solvent system they concluded that the reactivity primarily depended on the solubility of the gold particles and alkynyl compounds. In a later report Williams *et al.* claimed that the conversion rate is more dependent on relative surface coverage with azide terminated alkanethiols, determined by quantitative FTIR spectroscopy, than on solvent and ligand length.[24] When the relative amount of azide-terminated ligands was lower, higher overall yields were obser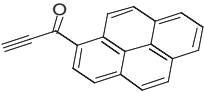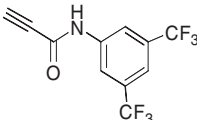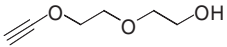ved. This phenomenon was attributed to steric interactions, leading to a reduced accessibility of azides as the click reaction progresses.

Sommer *et al.* showed that a catalyzed click reaction could be performed on the same type of gold nanoparticles under microwave conditions, which allowed the reaction times to be kept under 10 min.[22] A mixture of dioxane–*t*-BuOH–H_2O (1:1:0.5) was used as solvent and $CuSO_4$–sodium ascorbate as the catalytic system. With these short reaction times particle aggregation caused by the catalyst appeared to be negligible. However, when

Table 11.1   *Acetylene containing (small) molecules attached to gold nanoparticles via cycloaddition reactions*

Without catalyst, yields 5–54%[23]	Without catalyst[25]	CuSO$_4$–Na ascorbate catalyst, MW, 10 min, yields 78–100%[22]

the particles were treated for more than 15 min particle aggregation was also observed. A variety of alkynes (Table 11.1) was clicked to the gold nanoparticles in a yield of 78–100%. In addition, Sommer and coworkers attached an *N*-heterocyclic carbene Pd complex to the gold nanoparticles and tested its catalytic activity in a Suzuki-type reaction. Using this
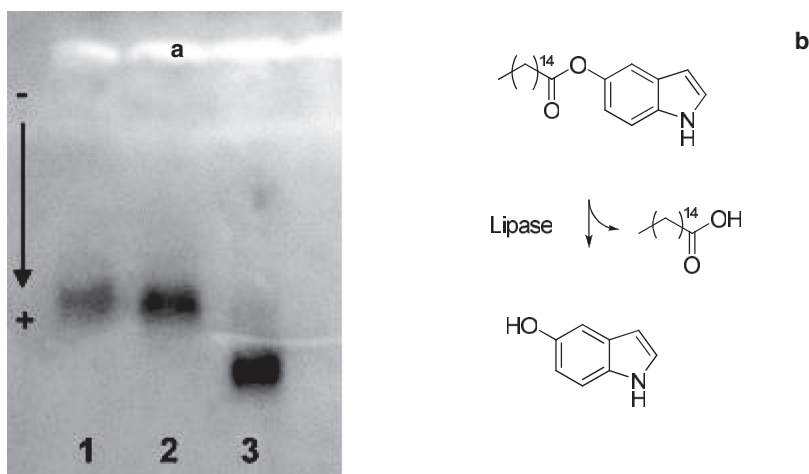
Figure 11.4 *(a) 1.5% agarose gel electrophoresis of AzNPs after click reaction. Lane 1: azide nanoparticles. Lane 2: azide nanoparticle-lipase reaction without copper. Lane 3: azide nanoparticle–lipase reaction with copper. (b) Hydrolysis of nonfluorescent ester, 5-O-palmitoylindole, to highly fluorescent 5-OH-indole. Reprinted with permission from ref.[26]. Copyright 2006 American Chemical Society.*

supported Pd catalyst a series of aryl chlorides was coupled with phenyl boronic acid in yields ranging from 85 to 99%.

Click reactions, however, can also be performed in water, thus gold nanoparticles coated with water-soluble ligand **15** were synthesized by Brust and coworkers.[26] They attached acetylene functionalized *thermomyces lanuginosus* lipase to azide-functionalized water-soluble gold nanoparticles. The lipase was genetically altered to express only one solvent-accessible lysine which was modified with carbodiimide chemistry to provide the required acetylene functionality. Subsequently, the click reaction was performed using $CuSO_4$–ascorbic acid. The gold nanoparticle–lipase conjugate was compared with two control samples by agarose gel electrophoresis to demonstrate the covalent connection of the lipase with the gold nanoparticles [Figure 11.4(a)]. The activity of the bound lipase was measured as function of the cleavage of nonfluorescent ester, 5-*O*-palmitoylindole, to highly fluorescent 5-OH-indole [Figure 11.4(b)]. Covalently attached to the gold nanoparticles the lipase retained its enzymatic activity. However, because the exact concentration of bound lipase per nanoparticle was unknown, the activity could not be compared with that of the free lipase. Reasoning the other way around, assuming that the activity is neither increased nor decreased upon binding, the lipase loading to the gold nanoparticle could be calculated. Based on the measured activity, the attachment of seven lipase molecules per nanoparticle was calculated.

In addition to spherical shaped gold nanoparticles, azide-functionalized gold nanorods of length to diameter ratio ∼5 were also used to attach enzymes, viz. trypsin.[30] Nanorods coated with poly(4-styrenesulfonic acid-*co*-maleic acid) sodium salt (PSS-*co*-PMA) were synthesized and the carboxylic acid groups were subsequently used to attach NH_2-PEG-N_3 with the use of EDC as coupling reagent. Using $CuSO_4$–ascorbic acid as catalyst the

nanorods were decorated with trypsin. The activity of this bioconjugate was determined by incubation with casein. The amount of tyrosine released is a measure for the activity of trypsin. Attached to the gold nanorod trypsin retained 57% of its biological activity compared with free trypsin. When trypsin was attached to the nanorods electrostatically or via direct EDC-coupling the activity was less then 20%. It should be noted, however, that in the latter two cases the poly(ethylene glycol) (PEG) linker was lacking, which provides more flexibility and thus increases the accessibility of trypsin.

In the above-mentioned studies, gold nanoparticles were successfully linked with enzymes and small molecules. A converse approach is to label larger structures with gold nanoparticles. Fischler *et al*. clicked azide functionalized gold nanoparticles with alkyne modified DNA strands.[28] To this end gold nanoparticles of approximately 3 nm coated with glutathione bisazide ligand **18** were synthesized. Acetylene functional DNA strands were obtained by replacing all thymine bases of a 294 base pair long fragment with alkyne-modified derivatives in a polymerase chain reaction (PCR) experiment. TBTA complexes of Cu(I) were used as catalyst in the click reaction to couple the gold nanoparticles to the DNA strand. In order to prevent cross-linking of the DNA strands as a result of the attachment of multiple DNA strands to one gold particle a 1000 fold excess of azide–gold nanoparticles was used. TEM images showed the nanoparticles to be equidistantly (2.8 ± 0.5 nm) assembled on the DNA (Figure 11.5). The shell of the gold particles and the DNA strand lack contrast in TEM and are therefore not visible. The spacing of the particles corresponded nicely with the expected value of twice the thickness of the shell, which is approximately 1.4 nm.

Vogge *et al*. synthesized gold nanorods with either acetylene (**17**) or azide functionalized ligands (**16**).[27] Applying a 1:1 concentration of the acetylene and azide rods in a Cu-catalyzed 1,3-dipolar cycloaddition reaction, chainlike assemblies were formed [Figure 11.6(a)]. This preferred end-to-end assembly of gold nanorods was previously observed by Caswell *et al*. and attributed to preferential ligand displacement at the (111) faces at the end of the rods.[31] If one of the functional rods was in excess compared to the other one, more complex assemblies were obtained. Zhou *et al*. used a mixture of azide functionalized gold nanoparticles and acetylene functionalized gold nanoparticles to visually detect Cu(II) ions.[29] They used gold nanoparticles **19** and **20** in a 1:1 ratio and added $CuSO_4$ to the
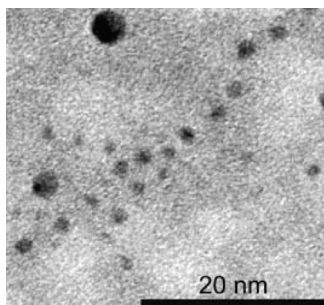

Figure 11.5 *TEM micrograph of one-dimensionally and equidistantly assembled gold nanoparticles on DNA immobilized on a TEM foil. Reprinted with permission from ref.[28]. Copyright 2008 Royal Society of Chemistry.*
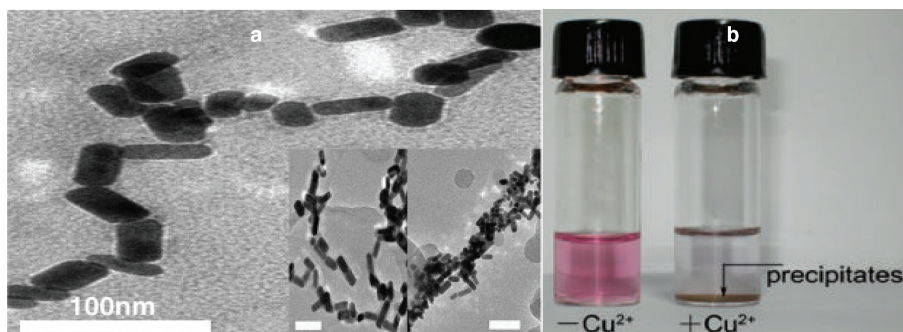
Figure 11.6   *(a) TEM pictures of chain like assemblies of gold nanorods obtained after the click reaction with 1:1 concentrations of nanoparticles **17** and **18**. Insert: the more complex assemblies if one of the compounds is present in excess. Reprinted with permission from ref.[27]. Copyright 2007 Elsevier. (b) Solution containing gold nanoparticles **19** and **20** before and after the addition of Cu(II) and sodium ascorbate. Reprinted with permission from ref.[29]. Copyright 2008 Wiley-VCH.*

red solution. As a result of the cross-linking of the particles the red color of the solution disappeared [Figure 11.6(b)].

With this assay Cu(II) ions could be detected with the naked eye down to a concentration of 50 μM. It was shown that the assay was insensitive to a variety of other metal ions and did not work without sodium ascorbate. Finally, 2.5 and 12 nm sized gold nanoparticles with acetylenes on their surface were conjugated with azide functionalized single walled nano tubes (SWNTs), as was demonstrated with electron microscopy (Figure 11.7).[32] The larger structures shown in Figure 11.7 were proposed to be bundles of SWNTs, since single SWNTs have a diameter of approximately 1 nm. The attached gold particles caused the semiconducting nanotubes to behave as conductors.

11.3   Carbon-based Nanomaterials

In the previous section was described how acetylene-labeled gold nanoparticles were conjugated with azide functionalized SWNTs. SWNTs are graphite-like allotropes of carbon

Figure 11.7   *Gold nanoparticles decorated with SWNTs via CuAAC: (a) 2.5 nm; (b) 12 nm. Reprinted with permission from ref.[32]. Copyright 2008 Institute of Physics.*

arranged in a cylindrical form; comparable allotropes arranged in a spherical form are referred to as fullerenes. Because of the versatile properties of SWNTs and fullerenes, they have often been utilized as molecular building blocks.

11.3.1 Fullerenes
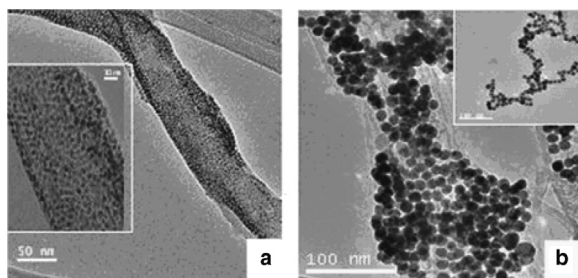
Fullerenes show a wide range of interesting chemical and physical properties which make them attractive objects of investigation. However, the range of suitable reactions that can be applied to functionalize fullerenes is relatively limited, because of their high reactivity toward nucleophiles and their appropriate 2π character for the application in cycloaddition reactions.[33] To prevent side reactions with fullerene conjugates, often the fullerenes are introduced in the final step of a process. This turned out to be challenging for both acetylene and azide functional fullerenes since purification of a mixture of fullerenes with a different number of functional groups is usually impossible.

Zhang *et al.* were able to functionalize a C_{60} fullerene with an acetylene via a Diels–Alder reaction with 2-trimethylsiloxy-1,3-butadiene, followed by reduction of the resulting cyclohexanone and subsequent esterification of the corresponding cyclohexanol (Scheme 11.6).[34] Using CuBr–PMDETA as catalyst acetylene-C_{60} was reacted with monofunctionalized polystyrene-azide (PS-N_3) of three different molecular weights (2, 6 and 10 kg mol^{-1}). These conjugates showed an unusual SEC behavior as depicted in Figure 11.8. Compared with unmodified 2 kg mol^{-1} PS-N_3 the retention volume of the fullerene conjugate was larger, as a result of which the molecular weight distribution appeared lower. For the 6 kg mol^{-1} polymer this observation was less obvious while the 10 kg mol^{-1} polymer did not show any such behavior. Apparently the C_{60} has a negative impact on the hydrodynamic volume of the polymer, especially in the case of the 2 kg mol^{-1} polymer. It was speculated that the lack of solubility of C_{60} in the solvent (THF) causes the polymer to shield the fullerene from the environment, which consequentially leads to a decreased hydrodynamic volume. In the case of the longer chains this effect is less significant.

To demonstrate that click reactions could be performed with fullerenes, Niergarten and coworkers prepared mono-acetylene, di-acetylene and di-azide functional C_{60} fullerenes.[35] Click reactions with either benzyl azide or 3-phenyl-1-propyne were utilized to functionalize these fullerenes. When the fullerenes did not dissolve well, side reactions (most probably cycloadditions of the azides to the fullerene core) were observed. These side reactions were

21   **22**
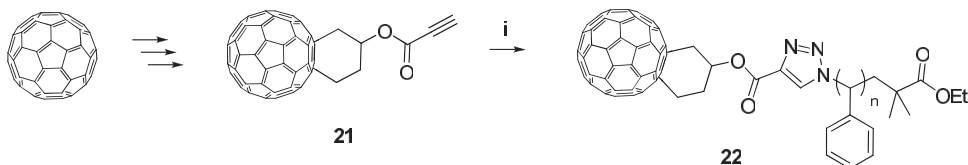
Scheme 11.6 *Modification of C_{60} with an acetylene group to acetylene–C_{60}* **21** *and subsequent click reaction with azide terminated PS to PS–C_{60}* **22**. *Reaction conditions: (i) CuBr, PMDETA, toluene, room temperature (r.t.).*[34]
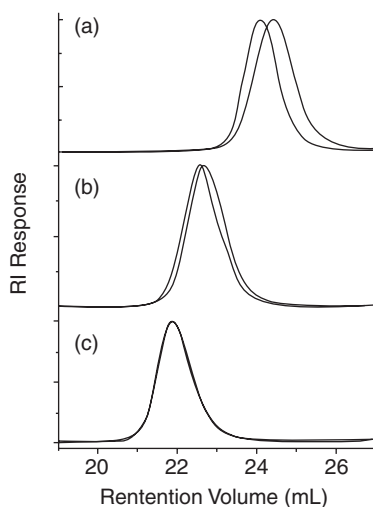
Figure 11.8   *Overlay of SEC traces of PS-N$_3$ and PS-C$_{60.}$ (a) M$_n$ = 2000; (b) M$_n$ = 6100; (c) M$_n$ = 10 000 for PS. Reprinted with permission from ref.[34]. Copyright 2008 American Chemical Society.*

reduced in the case of the fullerene bis-adduct because of its lower chemical reactivity. Niergarten also linked azides with acetylene fullerenes; mono-acetylene fullerene was attached to a di-azide fullerene and the expected triple fullerene conjugate was obtained according to mass spectrometry. Besides mono- and di-functional fullerenes a symmetrical addition pattern of C$_{60}$ is also possible (the octahedral addition pattern with six adducts). Most previously reported C$_{60}$ hexakis adducts were prepared via a one-pot synthesis using cycloaddition reactions with malonates. For small molecules this is an effective procedure, but for more complex structures yields are often found to be low. Therefore, fullerene hexakis-adducts with an octahedral addition pattern were prepared (Scheme 11.7), containing two azides per adduct, hence 12 in total.[36] With azides present on the fullerene six different acetylene-containing molecules, including a Zn(II)-porphyrin, were grafted to the fullerene in 12-fold with yields ranging from 56 to 81%.

In biological molecular recognition events the multivalent display of saccharides is an important principle. Such a multivalent display of functional groups can be achieved in a straightforward manner starting from fullerenes. Shiga-like toxins for example were shown to be neutralized efficiently by a pentavalent, water-soluble carbohydrate.[37] The AB$_5$ shiga-like toxins are produced by *Escherichia coli* serotype O157:H7 and cause dysentery in humans. Shiga-like toxin is built up from one A subunit responsible for its toxicity and five B subunits arranged in a C_5-symmetrical way for recognition of specific cell types. Isobe *et al*. have reported a C_5-symmetrical fullerene functionalized with five monosaccharides via sulfide linkages.[38] When they wanted to apply their methodology to larger saccharides the reaction was sluggish and many by-products were formed. To overcome this problem they synthesized a fullerene-bearing five acetylene moieties.[39] This C_5-symmetric acetylene C$_{60}$ was attached to a variety of molecules including a trisaccharide using the CuAAC reaction. Under the mild click conditions yields of 86% were achieved.
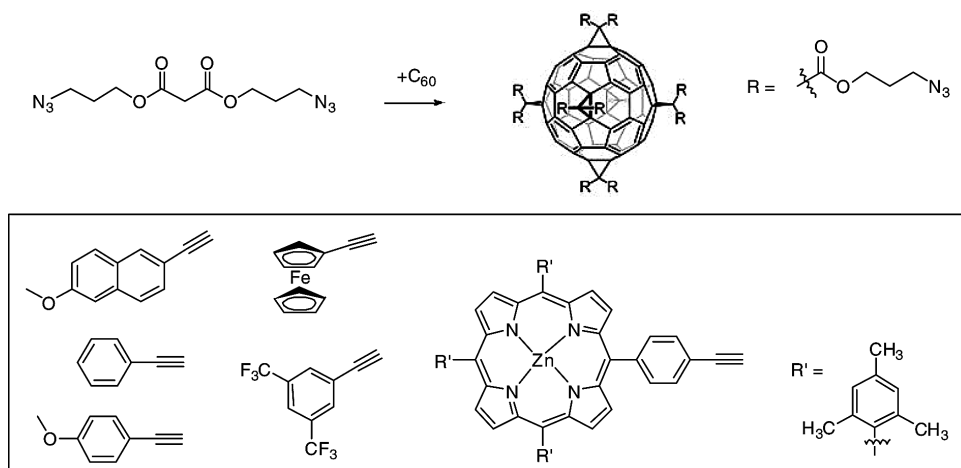
Scheme 11.7   *Functionalization of C_{60} with 12 azides in an octahedral addition pattern and the acetylene molecules applied in the click reaction.[36]*

The obtained penta-trisaccharide is expected to be an effective receptor for shiga-like toxin (Figure 11.9).

11.3.2   Carbon Nanotubes

Single walled carbon nanotubes are cylindrical sheets of graphite with a diameter of usually several nanometers and a possible length of up to several milimeters.[40] SWNTs are among the stiffest and strongest fibers known and possess remarkable electronic properties along
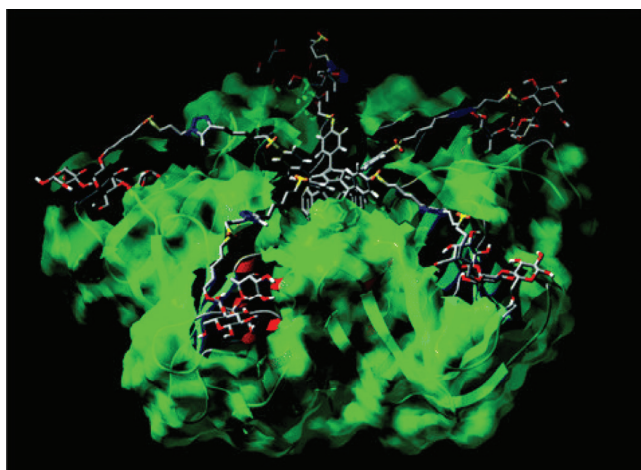

Figure 11.9   *Molecular model of shiga-like toxin (the molecular surface shown in green) complexed with a C_{60} trisaccharide conjugate (stick model).[39]*

with other unique characteristics, for example SWNTs can be semi-conducting or metallic depending on the rearrangement of their hexagon rings. In the section on metal nanoparticles it has already been described how SWNTs were coupled to gold nanoparticles via the Huisgen cycloaddition reaction.

Because of their graphite-like structure, SWNTs are insoluble in most organic and aqueous solvents. Much research effort has been put into trying to overcome this problem. Adronov and coworkers have used the click reaction to graft azide–PS on acetylene-SWNTs (Scheme 11.8) in order to increase solubility in the solvents in which PS is soluble.[41] Reactions were catalyzed with $(PPh_3)_3CuBr$ or CuI–1,8-diazabicyclo[5.4.0-undec-7-een] (DBU) in DMF; the system with CuI–DBU gave the best results. After treating this PS–SWNT conjugate with acetyl sulfate the material dissolved in water.[42] To demonstrate their increased solubility SWNT-PS and SWNT-sulfonated-PS (SWNT-PSS) were dissolved in an H_2O–DCM mixture; Figure 11.10 shows that SWNT-PS dissolves in DCM and SWNT-sulfonated-PS in H_2O.

Moreover, cyclodextrins (CDs) were successfully applied by Zheng *et al*. to functionalize SWNTs. The CD-SWNTs were prepared using CuI–DBU in DMF as solvent (Scheme 11.8).[43] Cyclodextrins are known to bind various organic and biological guests within their hydrophobic cavity in aqueous solution and CD-SWNTs hybrids are therefore anticipated as interesting supramolecular building blocks. To test the binding ability of the covalently linked CDs, the association of quinine with the CD-SWNTs was examined by fluorescence spectroscopy. As can be seen in Figure 11.11, the fluorescence of quinine was quenched upon the addition of the CD-SWNTs, indicating binding of the CD-SWNTs to quinine.

Phthalocyanines are planar electron-rich aromatic macrocycles that possess remarkably high extinction coefficients in the red/near-infrared region. A combination of such an electron donor molecule with the electron accepting carbon framework of SWNTs might lead to new photoactive materials. Such materials are potentially applicable in the development of, for example, efficient photovoltaic cells. Campidelli *et al*. applied $CuSO_4$–sodium ascorbate to react azide zinc–phthalocyanine (ZnPc) with acetylene–SWNT to obtain a single SWNT–ZnPc conjugate **23** (Scheme 11.8).[44] To test the photovoltaic properties of the complex, SWNT–ZnPc conjugate **23** was deposited on indium tin oxide (ITO)-coated glass slides. These glass slides were built into a photoelectrochemical cell as depicted in Figure 11.12. Reproducible photocurrents with monochromatic incident photon-to-current conversion efficiency (IPCE) values of 17.3% were measured for the SWNT–ZnPc conjugate. The monochromatic IPCE value for SWNTs coated with trimethylsilyl-protected 4-ethynylbenzene (a precursor for the SWNT-ZnPc conjugate) was more than 50% less.

Another class of graphite-like structures was prepared by Mynar *et al*. They made a graphitic diblock nanotube with an azide-covered surface via self-assembly of compound **24** (Figure 11.13).[45]

The diblock nanotubes were attached to dendron **25** via the CuAAC reaction as a suspension in THF–MeOH–hexane. AFM images showed that the diameter of dendron conjugated assemblies increased 4 nm compared to the nonfunctionalized nanotubes. The size of the dendron is roughly 2 nm and therefore this observation indicates that the exterior of the graphitic diblock nanotube is fully occupied with dendron **25**.
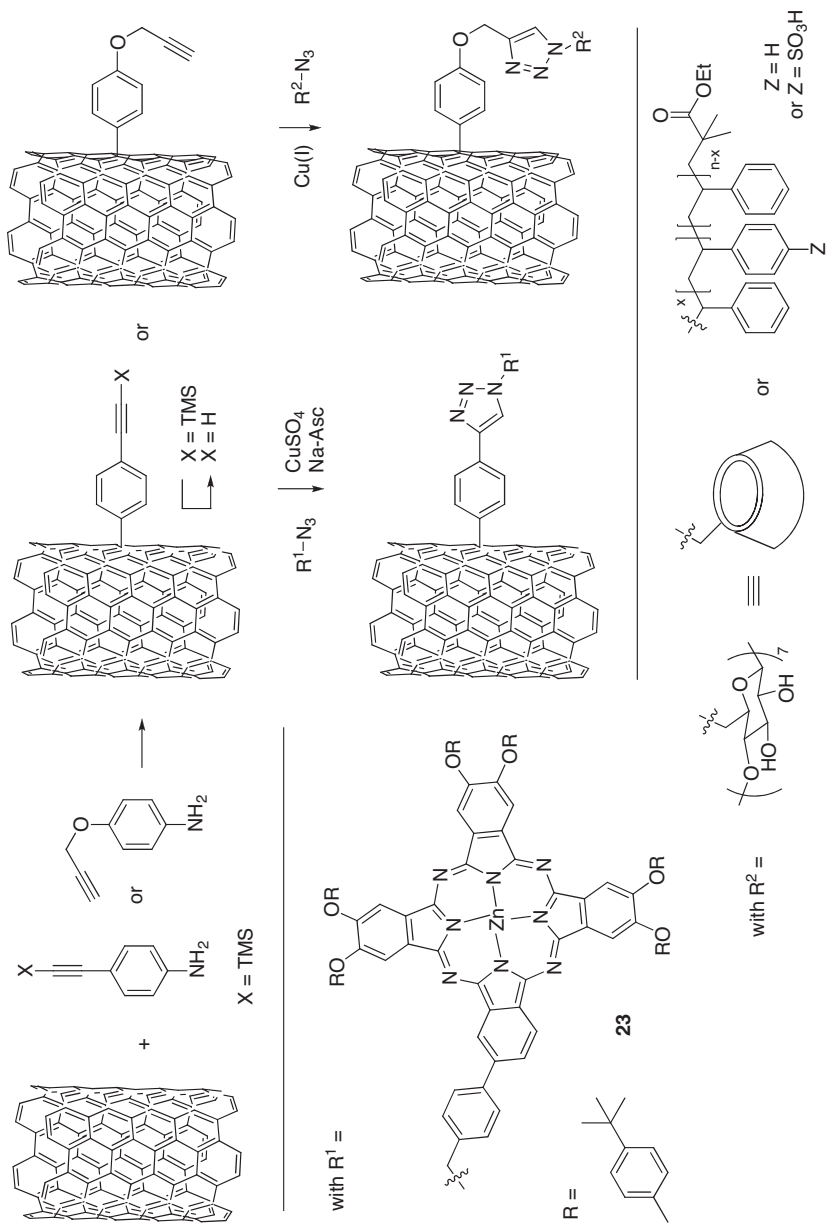
Scheme 11.8 *Functionalization of SWNTs with alkyne moieties and subsequent click reaction with azido-zinc-phthalocyanine,[44] azido-PS, azido-PSS[42] and azido-β-cyclodextrin.[43]*
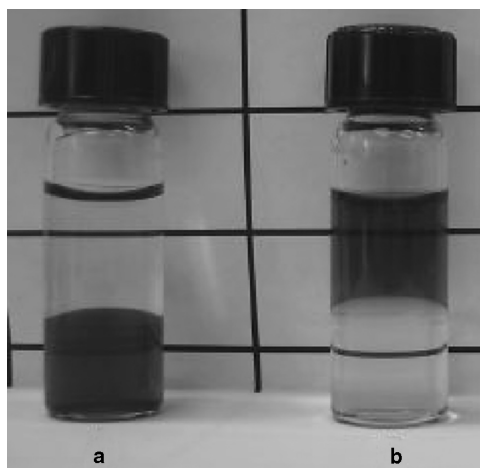
Figure 11.10 *Photograph of two separate SWNTs samples in CH₂Cl₂–H₂O. (a) Polystyrene functionalized SWNTs; (b) sulfonated polystyrene functionalized SWNTs. Reprinted with permission from ref.[42]. Copyright 2007 Elsevier.*
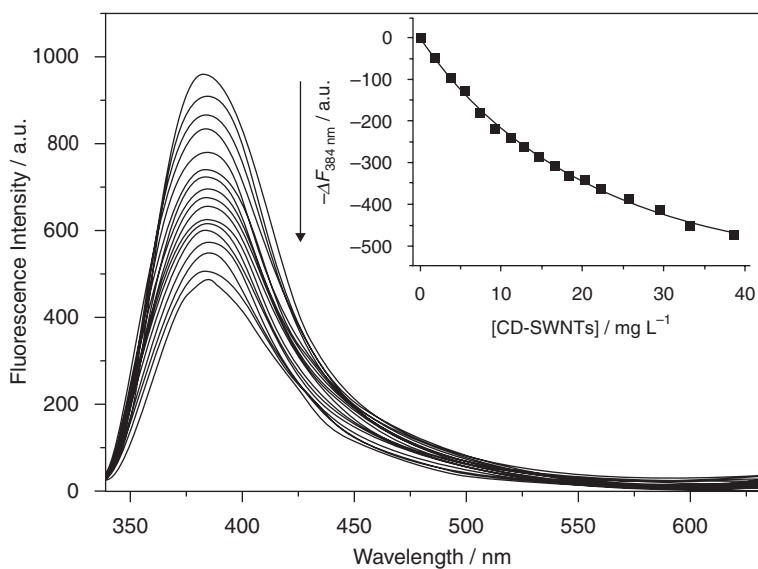
Figure 11.11 *Fluorescence spectral changes of quinine ($2.34 \times 10^{-5}\,mol\,l^{-1}$) upon addition of CD-SWNTs (0–39 mg l^{-1} from top to bottom) in aqueous buffer solution (pH = 7.4, 25 °C). Insert: differential fluorescence intensity (ΔF) vs the concentration of CD-SWNTs relationship. The excitation wavelength is 330 nm. Reprinted with permission from ref.[43]. Copyright 2008 Springer Science and Business Media.*
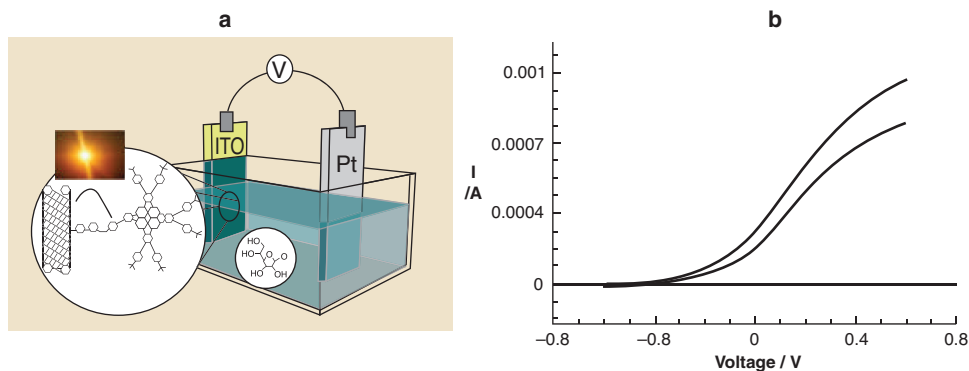
Figure 11.12 *(a) Schematic representation of the photoelectrochemical cell used for the IPCE measurements. (b) I–V characteristics of the SWNT–ZnPc conjugate under white light illumination, gray line, and in the dark, black line. Three-electrode setup, 0.1 M Na$_3$PO$_4$, 1 mM sodium ascorbate, N$_2$ purged. Voltages measured vs an Ag–AgCl reference electrode (0.1 M KCl). Reprinted with permission from ref.[44]. Copyright 2008 American Chemical Society.*

11.4 Self-assembled Organic Structures

In addition to the self-assembled nanotubes described in the previous section, here the functionalization of different types of self-assembled organic structures is surveyed. Huisgen cycloaddition reactions performed to functionalize liposomes, polymersomes and polymer
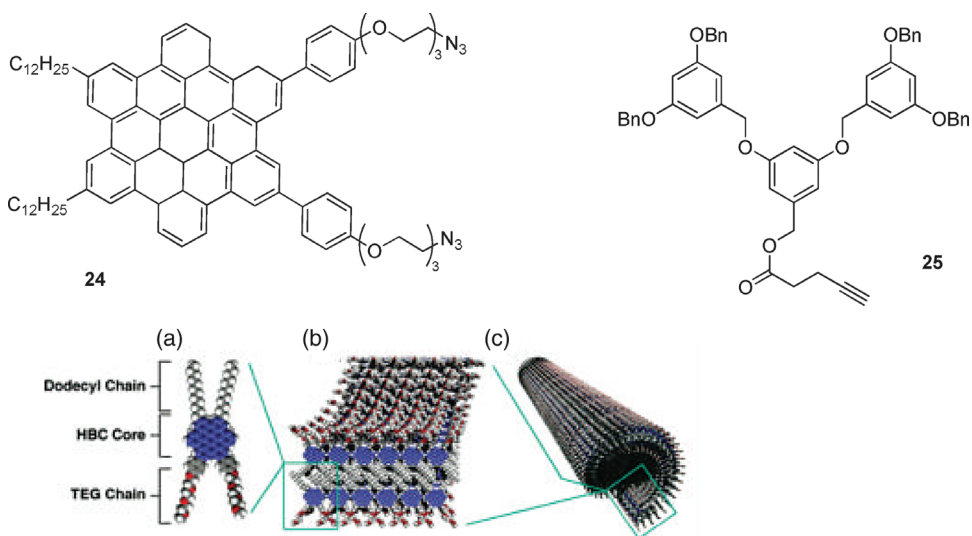
Figure 11.13 *Schematic structures of (a) 24, (b) self-assembled bilayer tape, (c) graphitic nanotube and structures of Hexa-peri-hexabenzocoronene (HBC) 24 and dendron 25. Reprinted with permission from ref.[45]. Copyright 2008 American Chemical Society.*
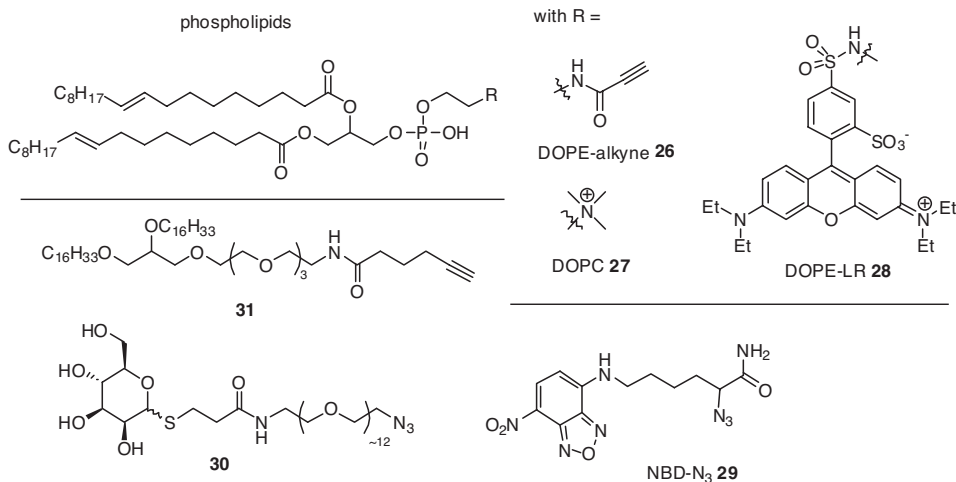
Scheme 11.9 *Structures of phospholipids **26**, **27**, **28** and **31**, NBD derivative **29** and mannose derivative **30**.[47,48]*

micelles will be discussed. Liposomes are structures similar to cells composed of an (aqueous) solution enclosed by a membrane. They are formed through self-assembly of naturally occurring phospholipids into a bilayer structure. Another example of amphiphilic molecules that can self-assemble are block-copolymers composed of a hydrophilic and a hydrophobic segment. They can assemble into, for example, polymersomes, the polymeric equivalent of liposomes, and polymeric micelles.

11.4.1 Liposomes

Surface modification of liposomes with for example peptides or proteins is used to obtain liposomes that can for instance be used for targeting to specific cells.[46] To perform surface modification of liposomes with the click reaction, Kros and coworkers prepared liposomes bearing alkyne groups at their surface.[47] This surface modification was done by preparing liposomes from a mixture of three different phospholipids, i.e. DOPE-acetylene (**26**), DOPC (**27**) and DOPE-LR (lissamine rhodamine) (**28**) (Scheme 11.9). The different phospholipids were mixed in a ratio of 50:49:1 DOPE-acetylene–DOPC–DOPE-LR. Unilamelllar liposomes (**32**) with an average diameter in the range of 110–120 nm were formed. Liposomes obtained with this procedure were attached to nitro-benzoxadiazole (NBD) derivative **29** via the Huisgen cycloaddition reaction using CuBr as catalyst. After attachment of **29** a Förster resonance energy transfer (FRET) effect between NBD and LR was observed, indicative that the modification occurred at the liposome surface. (Scheme 11.10). In the control sample without a copper catalyst only a minor FRET effect was observed, probably due to random presence of the NBD.

Hassane *et al*. prepared acetylene containing liposomes **33** (Scheme 11.10) from DPPC, DPPG, cholesterol and 5–10 mol% acetylene modified lipid **31** (Scheme 11.9).[48] The obtained liposomes were clicked with azido-mannose **30** using $CuSO_4$, sodium ascorbate and bathophenanthroline disulfonic acid disodium salt (BPhT) as catalyst system.
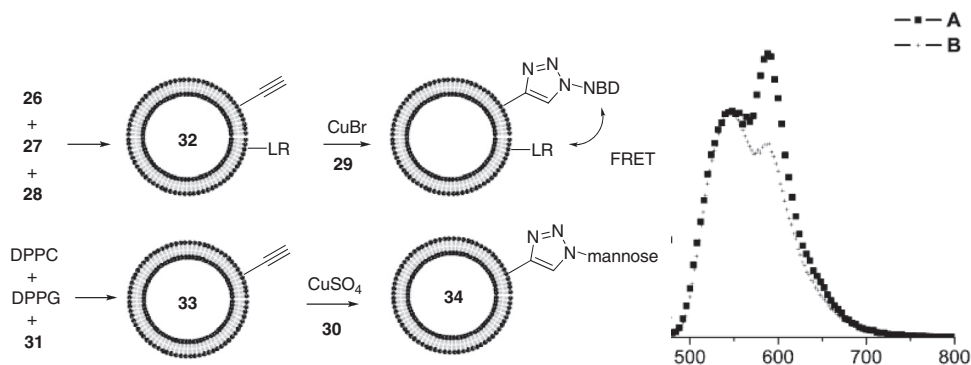
Scheme 11.10 *Top left: CuAAC reaction of LR and acetylene functional liposomes with NBD-derivative **29**. Right: FRET (excitation λ = 470 nm) spectra (**A** with CuBr and **B** for negative control without CuBr).[47] Bottom left: Attachment of azido-mannose **30** to liposome **33**.[48]*

To determine the mannose accessibility when conjugated to the liposome surface, concanavalin A (ConA), a sugar binding protein, was added. After addition of ConA to liposomes **34** in HEPES-buffered saline (HBS) (pH 6.5), an increase in turbidity was observed which was assessed by measuring the increase in optical density at 360 nm. Addition of unbound mannose resulted in immediate decrease in turbidity. This phenomenon was not observed for control liposomes lacking mannose.

11.4.2 Polymersomes

Polymersomes are architectures formed by self-assembly of amphiphilic block copolymers into bilayer structures that bear a resemblance to liposomes. Polymersomes, however, show a much greater stability compared with their low molecular weight counterparts.[49]

Van Hest and coworkers synthesized a diblock copolymer of poly(acrylic acid) (PAA) and polystyrene (PS) terminated with an azide group at the PAA side (Scheme 11.11).[50] After self-assembly of amphiphilic block copolymer **35**, polymersome **36** was formed with azide groups present at its periphery.

Azide containing polymersome **36** was further functionalized with various acetylene-containing substrates. Using TBTA or BPhT as ligands for the Cu(I) catalyzed cycloaddition, dansyl-acetylene was conjugated to the azide polymersomes. To measure the degree
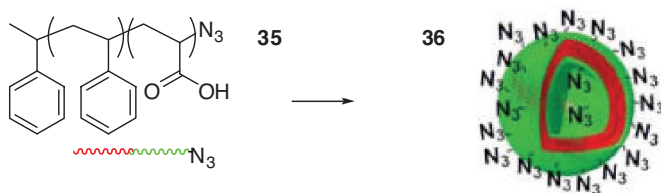
Scheme 11.11 *Structures of copolymer **35** (PS-b-PAA) and azide containing polymersome **36**.[50]*
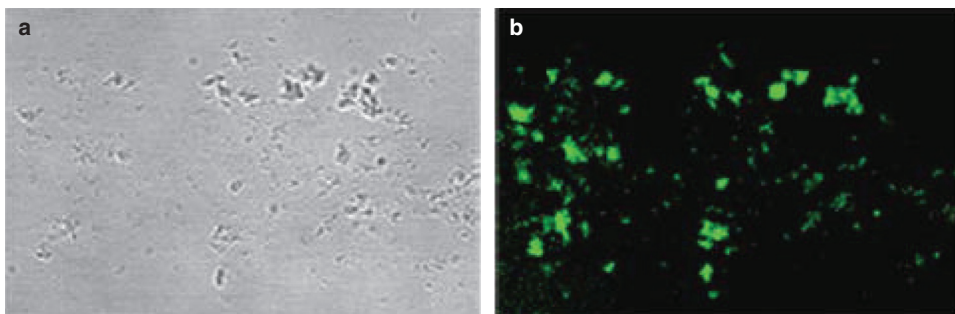
Figure 11.14 *Confocal laser-scanning microscopy images [transmission (A) and fluorescence excited at 488 nm (B)].*[50]

of functionalization, a reference compound (dansyl-PAA-*b*-PS) was synthesized. By comparison of the fluorescence of re-dissolved polymersomes and the reference compound it was calculated that about 23% of all azides were converted. Since the interior azides are unavailable for reaction, approximately 40–50% of the theoretical available azide-groups had reacted. To prove that the dansyl was really covalently attached, SEC traces of the re-dissolved block copolymers were recorded. After conjugation with dansyl the block copolymers were detected at 345 nm whereas unreacted block copolymer **35** did not give a signal at this wavelength.

Under the same conditions, enhanced green fluorescent protein (EGFP) was clicked to azido-polymersomes **36**. EGFP was equipped with acetylenes by reaction of pentynoic acid *N*-succinimidyl ester with one or more of the 20 available lysine residues. The EGFP-polymersomes showed fluorescence, which was detected by confocal laser scanning microscopy (Figure 11.14). When copper was omitted, the polymersomes did not show any fluorescence after dialysis.

Additionally, van Hest and coworkers designed an acetylene-PEG-*b*-PS block copolymer for the co-aggregation into PS-*b*-PIAT {polystyrene-poly[L-isocyanoalanine(2-thiophen-3-yl-ethyl)amide]}-based polymersomes.[51] Polymersomes prepared from PS-*b*-PEG or PS-*b*-PAA have the advantage that they are easily post modified. However, polymersomes based on these polymer constructs are impermeable for most organic substrates. PS-*b*-PIAT-based polymersomes, in contrast, are permeable for organic substrates. To obtain acetylene functionalized PS-*b*-PIAT polymersomes, acetylene-PEG-*b*-PS was co-aggregated into its bilayer membrane. Based on a calibration curve measured with SEC, the incorporation efficiency of acetylene-PEG-*b*-PS into PS-*b*-PIAT polymersomes was calculated to be 85%. Finally, an azido-functional lipase (azido-CalB) was clicked to acetylene polymersomes in the presence of $CuSO_4$, sodium ascorbate and bathophenanthroline. Hydrolysis of 6,8-difluoro-7-hydroxy-4-methylcoumarin octanoate (DiFMU octanoate) by *Candida antarctica* lipase B (CalB), yielding fluorescent difluoro-coumarin, was used to check the protein's activity.[52] CalB polymersomes showed the expected enzymatic activity whereas control experiments did not (Figure 11.15).

Another type of polymersome was constructed by Li *et al.*, by mixing azide-terminated polybutadiene-*b*-poly(ethylene oxide) (PBD-*b*-PEO-N_3) with hydroxyl terminated PBD-*b*-PEO-OH to obtain azide functional polymersomes.[53] These polymersomes were
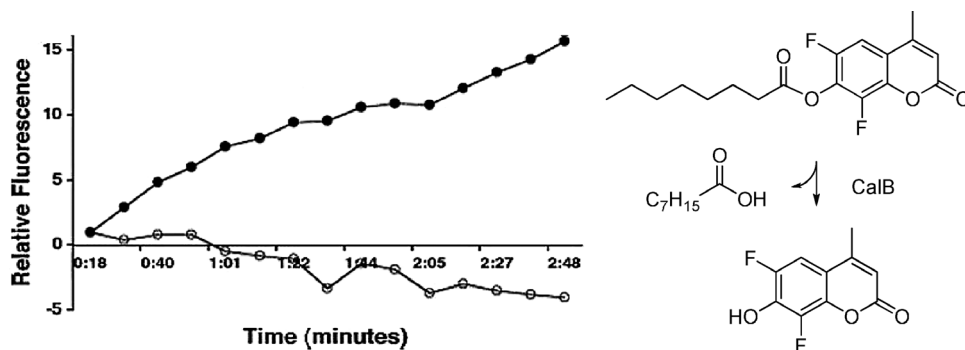
Figure 11.15 *Activity measurement of azido-functional CalB conjugated to a polymersome surface (●) compared with a blank experiment where acetylene-PEG-b-PS was not embedded in the polymersomes (○), via monitoring the hydrolysis of DiFMU octanoate to yield fluorescent difluoro-coumarin. Reprinted with permission from ref.[52]. Copyright 2008 Wiley-VCH.*

subsequently attached to an acetylene functional polyester dendron via the CuAAC reaction (Figure 11.16). To prove that the dendron was covalently attached, it was modified with a rhodamine derivative before performing the click reaction. This modification was done in such a way that approximately one rhodamine moiety was introduced per dendron. The yield of the conjugation was measured as a function of the PBD-*b*-PEO-N$_3$ concentration relative to PBD-*b*-PEO-OH. Again 50% of PBD-*b*-PEO-N$_3$ was expected to be inaccessible at the polymersome interior.

At low concentrations the conjugation yields were higher, as anticipated based upon the expected accessibility and crowdedness. The authors suggested that some of the interior azides had moved to the surface during the 24 h course of the reaction. Typically, increasing the amount of azide block copolymer in the mixture gave a decreased conjugation yield,

Figure 11.16 *Polyester dendron labeled with approximately one rhodamine moiety per molecule.[53]*

probably due to steric hindrance between the dendrons. Moreover, a deformation could be observed for polymersomes containing more than 40% of the azide amphiphile.

11.4.3   Micelles and Cross-linked Nanoparticles

As mentioned in the introduction of this chapter, besides polymersomes, amphiphilic block copolymers can also assemble into polymeric micelles. When polymeric micelles are cross-linked, well-defined and stable nanoparticles emerge. The dimensions and other properties of these cross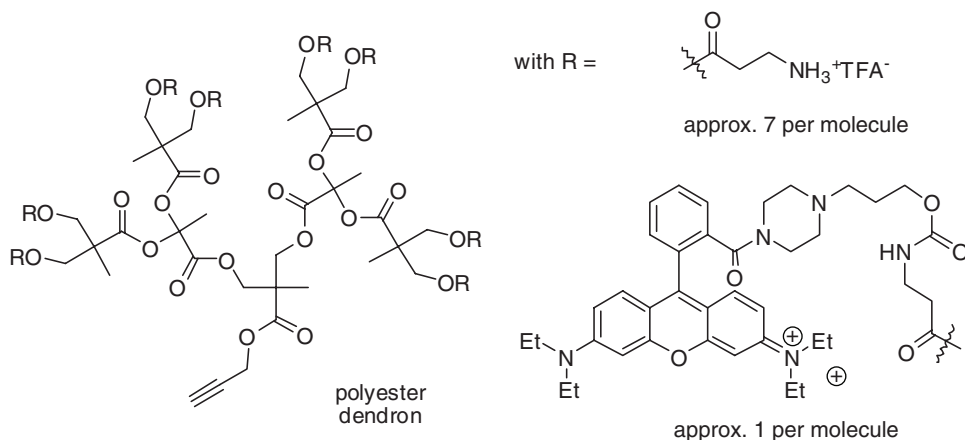-linked nanoparticles can easily be altered by changing the amphiphilic block copolymer properties. Polymeric micelle systems have attracted a lot of interest, e.g. as drug delivery vehicles or nanoreactors.[54]

Wooley and coworkers prepared micelles **38a–b** from PAA-*b*-PS **37** and used the PAA block for cross-linking and the introduction of azides or acetylenes (Scheme 11.12).[55] Block copolymer **37** was synthesized via consecutive nitroxide-mediated polymerization of *tert*-butyl acrylate and styrene. Afterwards the *tert*-butyl esters were removed with tri-fluoro acetic acid in dichloromethane. Micelles were formed by addition of water to a solution of the block copolymer in THF. After the formation of micelles, either azides (**38a**) or acetylenes (**38b**) were introduced to the micelle shell by EDC-coupling of respectively 3−azidopropylamine or propargylamine to the carboxylic acid functionalities of the PAA. The nanoparticles were subsequently shell cross-linked through amidation with 2,2′−(ethylenedioxy)bis(ethylamine). The authors showed that azide or acetylene functional fluorescein could be covalently linked to the cross-linked shell with the appropriate functionality through the Cu-catalyzed Huisgen cycloaddition reaction.

To prove that the fluorescein was linked covalently, a purified sample was centrifuged at 5000 rpm and emission spectra were recorded at different positions across the cell. The expected absorption maximum was only visible at the cell bottom and not at the middle or top. For the authors this was indicative that there was no free dye in solution and thus the dye was bound covalently to the cross-linked micelles.

To introduce azides or acetylenes to the core, the PS block was modified.[55,56] The incorporation of azides to the core was achieved via polymer **39** and after assembly into micelles the chlorides were replaced with azides. Acetylene functional core micelles were prepared via polymer **40**, which was deprotected to polymer **41** and subsequently self-assembled. Using the CuAAC reaction acetylene dansyl was conjugated with micelle **42a** and azide coumarin was attached to **42b**; in both cases IR and NMR spectroscopy confirmed a covalent attachment to the coronas.

Acetylene functional micelles were also shell cross-linked[57] and core cross-linked[58] via the 1,3-dipolar cycloaddition reaction with azide dendrimers by Wooley and coworkers. Micelles **38b** and **42b** were prepared and were subsequently subjected to click reactions with the azide dendrimers shown in Scheme 11.13. After the addition and subsequent purification by dialysis, dynamic light scattering (DLS) showed that the size of cross-linked particles was independent of concentration and temperature. Furthermore, it was shown the shell was only effectively cross-linked with the first-order dendrimer whereas the core was cross-linked for all dendrimer generations. It was suggested that the hydrophobic nature of the dendrimers prevented efficient cross-linking of the hydrophilic shell.

Functionalities introduced at the shell or in the core of polymer micelles are likely to be sterically and electronically hindered. To mimic a more solution-like environment
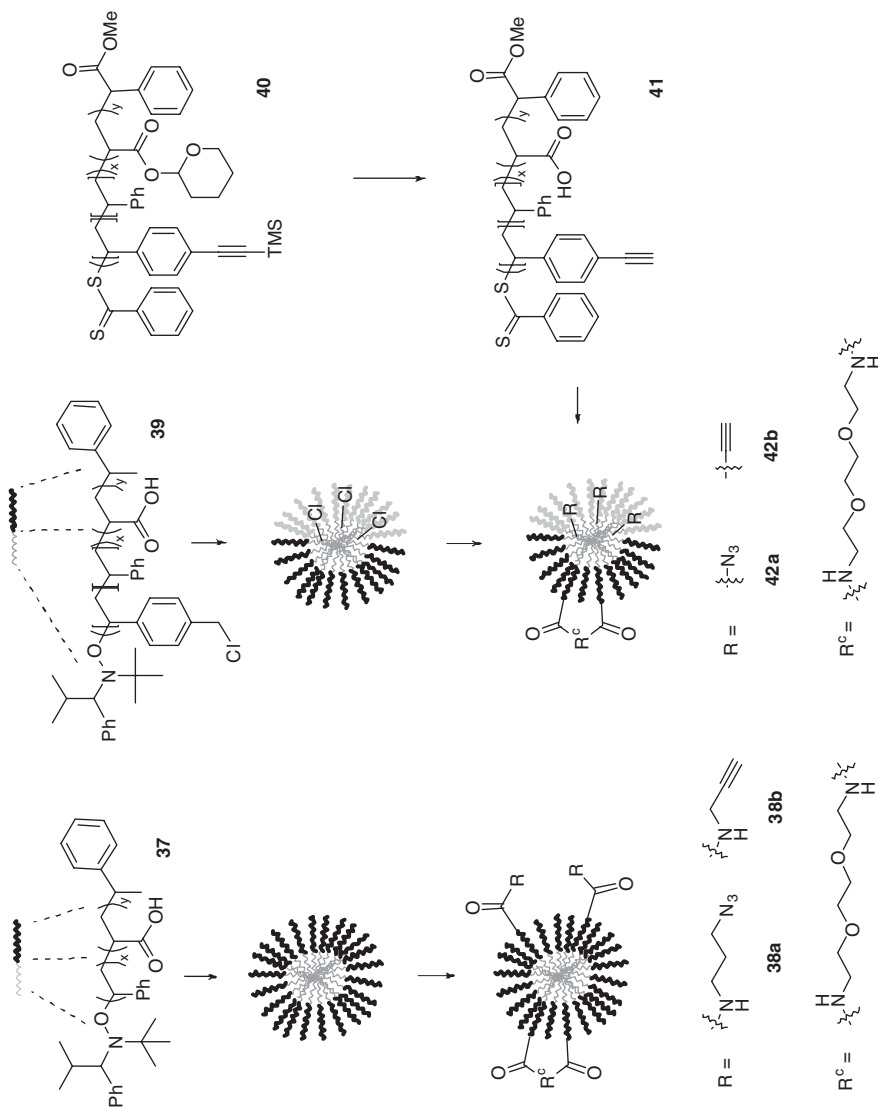
Scheme 11.12 *Preparation of cross-linked micelles functionalized in their shell with azides 38a or acetylenes 38b and functionalized in their core with azides 42a and acetylenes 42b.*[55–57]
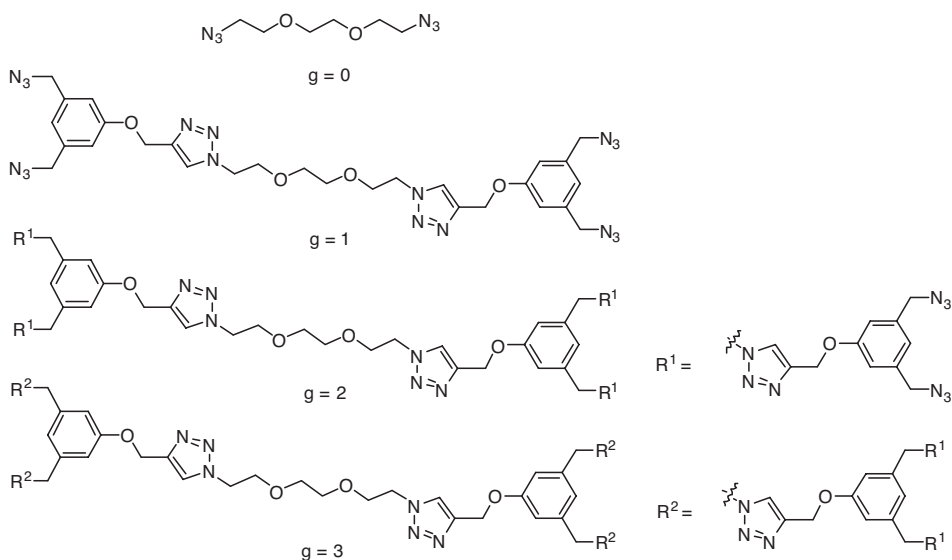
Scheme 11.13   *Dendrimers of generation (g) 0–3 used to cross-link polymeric micelles* **38b** *and* **42b**.[57]

attachment should only occur at the hydrophilic termini of the block copolymers. Therefore, PAA-*b*-PS block copolymers terminated with azide or acetylene functionalities at the PAA chain ends were synthesized (not shown).[59] Azide-terminated copolymers were prepared via a nitroxide-mediated polymerization, using a chloride-functional initiator, of which the chloride was subsequently replaced by an azide. Acetylene copolymers were obtained with a controlled RAFT polymerization starting with an acetylene functional initiator. Micelles were prepared from mixtures of the copolymers with and without functional termini, which were subsequently cross-linked through amidation and decorated with fluorescein dye molecules using the CuAAC reaction. The fluorescence intensity depending on pH was measured for both the free alkyne-functional fluorescein and fluorescein attached to azide micelles from which the authors concluded that fluorescein conjugated to the termini behaves as if free in solution.

Jiang *et al*. described the cross-linking via the click reaction of poly(*N,N*-dimethyl-acrylamide)-*b*-poly(*N*-isopropylacrylamide-*co*-3-azidopropylacrylamide)   [PDMA*b*-(NIPAM-*co*-AzPAM)] **43** (Scheme 11.14).[60] The NIPAM-*co*-AzPAM block is a thermo-responsive polymer with a lower critical solution temperature (LCST). Above the LCST, the NIPAM-co-AzPAM segment of block copolymer **43** starts to aggregate and micelles with a NIPAM-*co*-AzPAM core form.

Cross-linking of the core was achieved via a click reaction of dipropargyl ether with the azides present in the micelle interior. To prove cross-linking, the optical density as a function of temperature was measured. Dissolved block copolymer showed a transmittance of about 100%, which decreased to approximately 80% above the aggregation temperature. The transmittance of the cross-linked micelles did not change over the measured interval, indicating their stability in this temperature range.
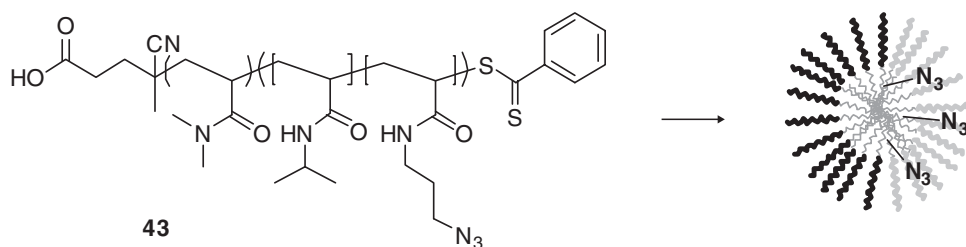
Scheme 11.14   *Thermo-responsive block copolymer* **43**.[60]

11.5   Virus Particles

The block copolymers from which polymersomes and polymer micelles are formed always show a distribution of molecular weight. Even if building blocks are monodisperse, like phospholipids, the self-assembled structures still display a distribution in size. The number of building blocks in liposomes, polymersomes or polymer micelles always varies, even under complete equilibrium conditions. Monodisperse building blocks are, however, encountered in biological systems in the form of proteins. Well-defined protein building blocks can assemble into highly organized 3D systems as is the case with virus particles. Virus particles contain a protein coat formed by self-assembly of proteins and exhibit an unparalleled monodispersity at this size scale. Virus particles are usually 50–300 nm in size and the plant viruses in particular are extremely suitable for modification and employable as well-defined biological nanoparticles.

   An example of a well defined and characterized, easily available virus is the Cowpea Mosaic Virus (CPMV). The CPMV particles are 30 nm in diameter and are formed by the assembly of 60 subunits around single-stranded viral genomic RNA. Each subunit is a complex of a large and a small protein of 42 and 24 kDa. Finn and coworkers decorated the CPMV capsid with azides or alkynes at either reactive lysine or cysteine residues (Scheme 11.15).[61]
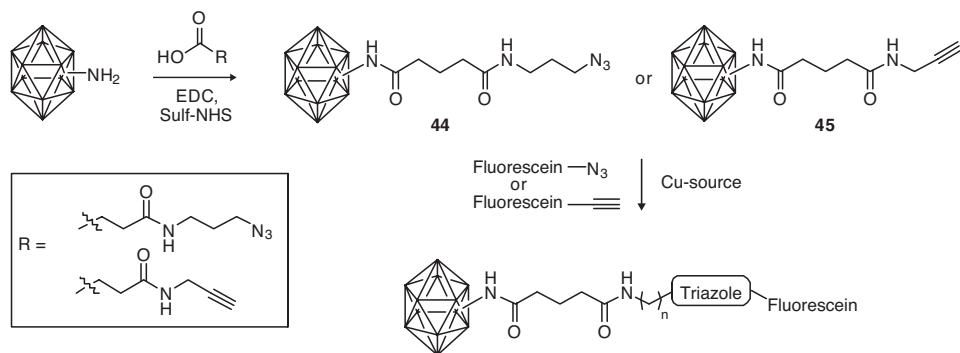
Scheme 11.15   *Preparation of azide- or acetylene-functionalized virus capsids.*[61]

Fluorescein derivatives with complementary functionality to the particles were used in a CuAAC reaction with $CuSO_4$–tris(triazole)amine, tris(carboxyethyl)phosphine (TCEP) and Cu wire as catalysts. Here TCEP was used as water-soluble reducing agent because addition of sodium ascorbate or *p*-hydroquinone as reductants resulted in disassembly of the virus capsids (later other conditions without TCEP were preferred[62–64]). Varying these conditions, a 100% conversion could be achieved for attachment of acetylene fluorescein to azide–CPMV and 80% was realized for the opposite combination. Independently, Wang and coworkers studied the attachment of various hemicyanine dyes using a similar approach.[65]

The Finn group reported optimized conditions for the click reaction to virus particles.[62] Using $Cu(MeCN)_4OTf$, $Cu(MeCN)_4PF_6$ or CuBr and sulfonated bathophenanthroline as catalyst, carbohydrates, peptides, poly(ethylene oxide) and transferrin were attached in high yields and substrate loadings. The carbohydrates were accessible when attached to CPMV, as was verified by the formation of a gel upon the addition of galectin-4. Peptides (KIRGDTFAGF and GLPLKDNYKK) were modified with an acetylene moiety for click reactions, and fluorescein to make them easy to detect. Sodium dodecyl sulfate–poly(acrylamide) gel electrophoresis (SDS–PAGE) analysis by UV irradiation showed modification of the particles with the selected peptides. This method for attachment of a fluorescent marker was also used to show the conjugation of PEG chains to the CPMV particles. Finally transferrin, an 80 kDa blood plasma protein for iron delivery, was attached to the virus particles via the cycloaddition reaction. TEM images showed an increase in particle size; the CPMV particles remained still intact after conjugation with transferrin (Figure 11.17).

Attachment of glycopolymers to, for example, a protein carrier could be a valuable tool in the study of carbohydrate-based cellular processes, which quite often depend on
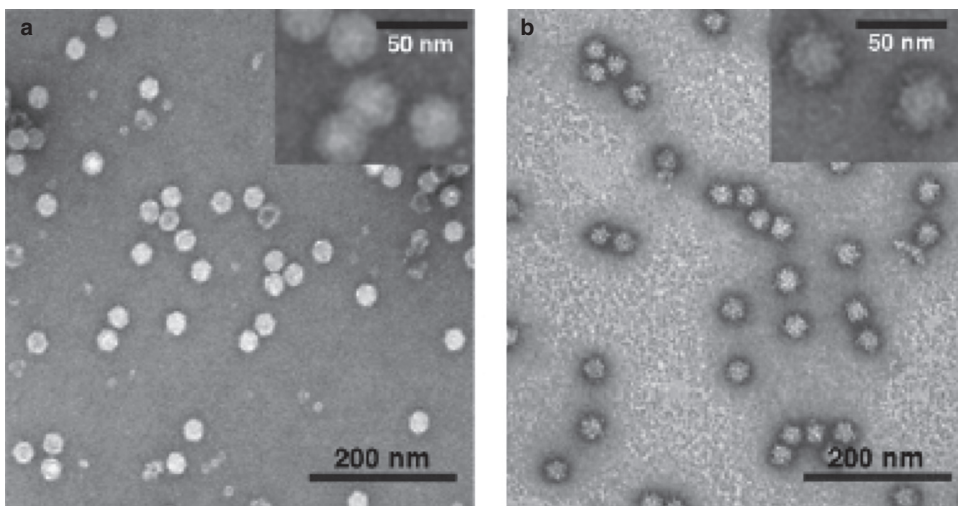

Figure 11.17 *(a) Negative-stained TEM of wild-type CPMV. (b) Negative-stained TEM of CPMV conjugated with transferrin. Automated measurement of the particles showed the average diameter to be 30 ± 1 nm for wild-type and 46 ± 5 nm for CPMV–transferrin. Reprinted with permission from ref.[62]. Copyright 2005 American Chemical Society.*
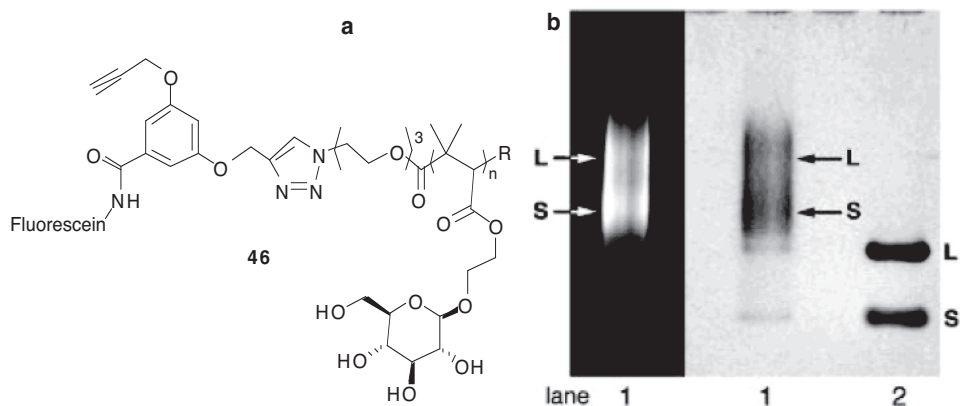
Figure 11.18 *(a) Glycopolymer prepared via ATRP. (b) SDS–PAGE of the glycopolymer conjugate (lane 1) and WT-CPMV (lane 2). The arrows mark the center of the bands derived from the small (S) and large (L) subunits; their broad nature derives from the polydispersity of the polymer and the possibility for more than one attachment of polymer per protein subunit. Reprinted with permission from ref.[63]. Copyright 2005 Royal Society of Chemistry.*

multivalency. Finn and coworkers synthesized glycopolymer **46** connected to a fluorescein moiety via atom transfer radical polymerization (ATRP) and conjugated it to CPMV particles via the CuAAC reaction using CuOTf–sulfonated bathophenanthroline as catalyst.[63] Figure 11.18 shows an SDS–PAGE gel of the glycopolymer–CPMV conjugates, demonstrating that both the large and small coat protein were functionalized with the glycopolymers (the broad bands arise from the polydispersity of the polymer). Besides glycopolymers, tetra- and hexasaccharides (e.g. globo-H) were also arrayed on the exterior surface of CPMV.[66] Particles coated with saccharides were injected into chickens to evaluate their IgY immune response. IgY was isolated from eggs and glycan-binding was determined on printed micro arrays containing 200 or 264 glycans.

Normal expression of the folate receptor (FR) in cells is low, but is upregulated in a variety of tumors. To target CPMV to a tumor cell with high FR expression poly(ethylene oxide)–folic acid was attached to CPMV particles **45**.[64] A PEG-spacer was incorporated to accomplish efficient cellular recognition of the folic acid (FA) units. CuOTf–sulfonated bathophenanthroline was used as catalyst for the click reaction. KB tumor cells (a human nasopharyngeal carcinoma cell line with high expression of FR) were incubated with different modified CPMV particles. Using flow cytometry an increased binding of CPMV-PEG-FA was established [Figure 11.19(a)].

Finally, CPMV particles conjugated with a gadolinium-tetraazacyclododecanetetraacetic acid Gd(DOTA) analog were prepared by Finn and coworkers.[67] Gd(DOTA) is a paramagnetic Gd complex used in magnetic resonance imaging as contrast agent. Acetylene functional Gd(DOTA) analog **47** [Figure 11.19(b)] was clicked with azide–CPMV **44** using Cu–bathophenanthroline as catalyst. With inductive coupled plasma optical emission spectrometry (ICP-OES), it was determined that 223 ± 20 Gd complexes were attached per CPMV particle.
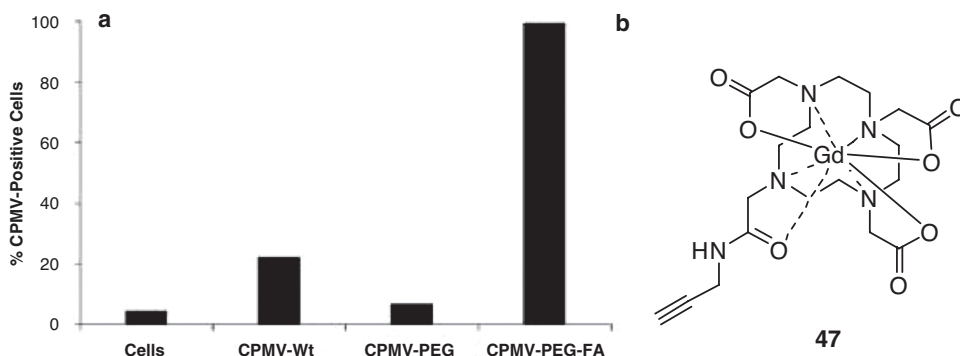
Figure 11.19 *(a) Percentage of increased binding of CPMV-PEG-FA to KB cells over controls. (b) Structure of acetylene functional Gd(DOTA). Reprinted with permission from ref.[64]. Copyright 2007 Elsevier.*

Another type of virus particle is the tobacco mosaic virus (TMV). TMV is a rod-like virus consisting of 2130 protein subunits arranged helically around genomic single RNA strands to form a 300 nm sized assembly. Francis and coworkers reported the exterior modification of TMV with diazonium coupling reactions.[68] Because this coupling procedure is difficult to apply using complex molecules, Bruckman *et al*. modified the exterior tyrosine molecules of TMV with the diazonium salt generated from 3-ethynylaniline *in situ* to obtain acetylene functional TMV.[69] Azide functional TMV was prepared by conjugating 1,4-bis-azidomethylbenzene to acetylene-TMV. A library of acetylene or azide functional (bio)molecules was successfully attached via the copper-catalyzed Huisgen cycloaddition reaction, see Scheme 11.16.

11.6   Conclusions

In this chapter the functionalization of a variety of nanoparticles with the copper-catalyzed Huisgen cycloaddition reaction between azides and alkynes has been described. The popularity of click chemistry in this field of science is based on its ease of execution, efficiency and orthogonality. Quite some examples can be found in which this method outperforms more traditional conjugation or functionalization procedures. It is also clear that there is still no general catalytic system, which requires an optimization of click conditions for each novel conjugation strategy. However, there are many opportunities ahead for functional particles prepared by the Huisgen cycloaddition reaction, also spurred on by new developments in the field. One such a recent development is the introduction of Cu-free click methods, which will further increase the application potential to areas such as microelectronics and the biomedical field, in which Cu is regarded as an undesirable impurity. Since most scientific achievements are of very recent date, it is clear that we have only witnessed the start of the effects click chemistry will have on the preparation of well-defined nanoparticles of both inorganic and organic origin.
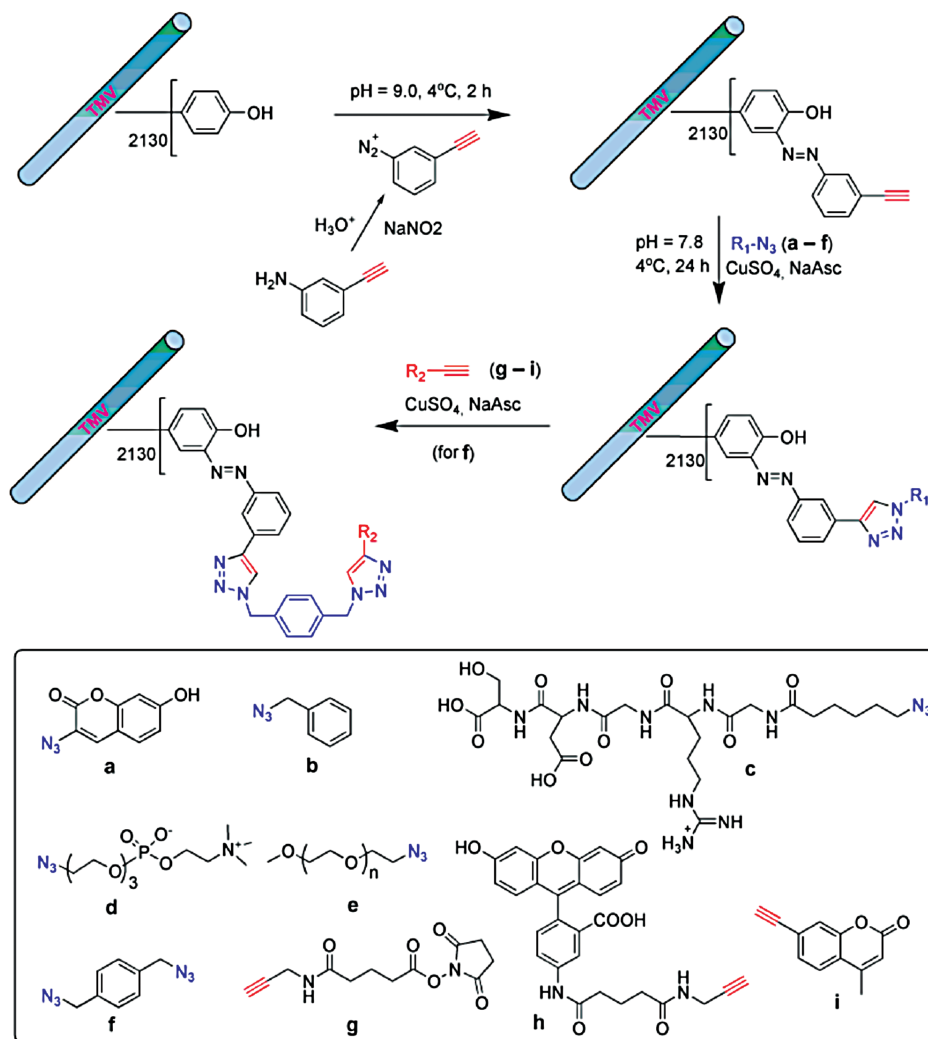
Scheme 11.16 *Bioconjugation of TMV by means of CuAAC reactions. Reproduced with permission from M. A. Bruckman, (2008), Surface modification of tobacco mosaic virus with 'click' chemistry,* ChemBioChem, ***9****, 519–523.*[69]

References

(1) C. Burda, X. Chen, R. Narayanan, and M. A. El-Sayed, (2005), Chemistry and properties of nanocrystals of different shapes, *Chem. Rev.*, **105**, 1025–1102.
(2) H. C. Kolb, M. G. Finn, and K. B. Sharpless, (2001), Click chemistry: diverse chemical function from a few good reactions, *Angew. Chem., Int. Edn*, **40**, 2004–2021.
(3) V. V. Rostovtsev, L. G. Green, V. V. Fokin, and K. B. Sharpless, (2002), A stepwise Huisgen cycloaddition process: copper(I)-catalyzed regioselective 'ligation' of azides and terminal alkynes, *Angew. Chem., Int. Edn*, **41**, 2596–2599.

(4) C. W. Tornøe, C. Christensen, and M. Meldal, (2002), Peptidotriazoles on solid phase: [1,2,3-triazoles by regiospecific copper(I)-catalyzed 1,3-dipolar cycloadditions of terminal alkynes to azides, *J. Org. Chem.*, **67**, 3057–3064.

(5) C. B. Murray, C. R. Kagan, and M. G. Bawendi, (2000), Synthesis and characterization of monodisperse nanocrystals and close-packed nanocrystal assemblies, *Annu. Rev. Mater. Sci.*, **30**, 545–610.

(6) H. Zou, S. Wu, and J. Shen, (2008), Polymer/silica nanocomposites: preparation, characterization, properties, and applications, *Chem. Rev.*, **108**, 3893–3957.

(7) B. Radhakrishnan, R. Ranjan, and W. J. Brittain, (2006), Surface initiated polymerizations from silica nanoparticles, *Soft Matter*, **2**, 386–396.

(8) R. Ranjan, and W. J. Brittain, (2007), Combination of living radical polymerization and click chemistry for surface modification, *Macromolecules*, **40**, 6217–6223.

(9) R. Ranjan, and W. J. Brittain, (2008), Synthesis of high density polymer brushes on nanoparticles by combined RAFT polymerization and click chemistry, *Macromol. Rapid Commun.*, **29**, 1104–1110.

(10) R. Ranjan, and W. J. Brittain, (2007), Tandem RAFT polymerization and click chemistry: an efficient approach to surface modification, *Macromol. Rapid Commun.*, **28**, 2084–2089.

(11) A. P. Alivisatos, W. Gu, and C. Larabell, (2005), Quantum dots as cellular probes, *Annu. Rev. Biomed. Eng*, **7**, 55–76.

(12) W. H. Binder, L. Petraru, R. Sachenshofer, and R. Zirbs, (2006), Synthesis of surface-modified nanoparticles via cycloaddition-reactions, *Monatsh. Chem.*, **137**, 835–841.

(13) W. H. Binder, R. Sachsenhofer, C. J. Straif, and R. Zirbs, (2007), Surface-modified nanoparticles via thermal and Cu(I)-mediated 'click' chemistry: Generation of luminescent CdSe nanoparticles with polar ligands guiding supramolecular recognition, *J. Mater. Chem.*, **17**, 2125–2132.

(14) S. Laurent, D. Forge, M. Port, A. Roch, C. Robic, L. Vander Elst, and R. N. Muller, (2008), Magnetic iron oxide nanoparticles: synthesis, stabilization, vectorization, physicochemical characterizations, and biological applications, *Chem. Rev.*, **108**, 2064–2110.

(15) M. A. White, J. A. Johnson, J. T. Koberstein, and N. J. Turro, (2006), Toward the syntheses of universal ligands for metal oxide surfaces: controlling surface functionality through click chemistry, *J. Am. Chem. Soc.*, **128**, 11356–11357.

(16) G. Lv, W. Mai, R. Jin, and L. Gao, (2008), Immobilization of dipyridyl complex to magnetic nanoparticle via click chemistry as a recyclable catalyst for Suzuki cross-coupling reactions, *Synlett*, 1418–1422.

(17) G. von Maltzahn, Y. Ren, J.-H. Park, D.-H. Min, V. R. Kotamraju, J. Jayakumar, V. Fogal, M. J. Sailor, E. Ruoslahti, and S. N. Bhatia, (2008), *In vivo* tumor cell targeting with 'click' nanoparticles, *Bioconjugate Chem.*, **19**, 1570–1578.

(18) P.-C. Lin, S.-H. Ueng, S.-C. Yu, M.-D. Jan, A. K. Adak, C.-C. Yu, and C.-C. Lin, (2007), Surface modification of magnetic nanoparticle via Cu(I)-catalyzed alkyne-azide [2 + 3] cycloaddition, *Org. Lett.*, **9**, 2131–2134.

(19) L. Polito, D. Monti, E. Caneva, E. Delnevo, G. Russo, and D. Prosperi, (2008), One-step bioengineering of magnetic nanoparticles via a surface diazo transfer/azide–alkyne click reaction sequence, *Chem. Commun. (Cambridge)*, 621–623.

(20) P.-C. Lin, S.-H. Ueng, M.-C. Tseng, J.-L. Ko, K.-T. Huang, S.-C. Yu, A. Kumar Adak, Y.-J. Chen, and C.-C. Lin, (2006), Site-specific protein modification through Cu(I)-catalyzed 1,2,3-triazole formation and its implementation in protein microarray fabrication, *Angew. Chem., Int. Edn*, **45**, 4286–4290.

(21) M.-C. Daniel, and D. Astruc, (2004), Gold nanoparticles: assembly, supramolecular chemistry, quantum-size-related properties, and applications toward biology, catalysis, and nanotechnology, *Chem. Rev.*, **104**, 293–346.

(22) W. J. Sommer, and M. Weck, (2007), Facile functionalization of gold nanoparticles via microwave-assisted 1,3 dipolar cycloaddition, *Langmuir*, **23**, 11991–11995.

(23) D. A. Fleming, C. J. Thode, and M. E. Williams, (2006), Triazole cycloaddition as a general route for functionalization of Au nanoparticles, *Chem. Mater.*, **18**, 2327–2334.

(24) C. J. Thode, and M. E. Williams, (2008), Kinetics of 1,3-dipolar cycloaddition on the surfaces of Au nanoparticles, *J. Colloid Interface Sci.*, **320**, 346–352.

(25) W. Limapichat, and A. Basu, (2008), Reagentless functionalization of gold nanoparticles via a 3 + 2 Huisgen cycloaddition, *J. Colloid Interface Sci.*, **318**, 140–144.

(26) J. L. Brennan, N. S. Hatzakis, T. R. Tshikhudo, N. Dirvianskyte, V. Razumas, S. Patkar, J. Vind, A. Svendsen, R. J. M. Nolte, A. E. Rowan, and M. Brust, (2006), Bionanoconjugation via click chemistry: the creation of functional hybrids of lipases and gold nanoparticles, *Bioconjugate Chem.*, **17**, 1373–1375.

(27) R. Voggu, P. Suguna, S. Chandrasekaran, and C. N. R. Rao, (2007), Assembling covalently linked nanocrystals and nanotubes through click chemistry, *Chem. Phys. Lett.*, **443**, 118–121.

(28) M. Fischler, A. Sologubenko, J. Mayer, G. Clever, G. Burley, J. Gierlich, T. Carell, and U. Simon, (2008), Chain-like assembly of gold nanoparticles on artificial DNA templates via 'click chemistry', *Chem. Commun. (Cambridge)*, 169–171.

(29) Y. Zhou, S. Wang, K. Zhang, and X. Jiang, (2008), Visual detection of copper(II) by azide- and alkyne-functionalized gold nanoparticles using click chemistry, *Angew. Chem., Int. Edn*, **47**, 7454–7456.

(30) A. Gole, and C. J. Murphy, (2008), Azide-derivatized gold nanorods: functional materials for 'click' chemistry, *Langmuir*, **24**, 266–272.

(31) K. K. Caswell, J. N. Wilson, U. H. F. Bunz, and C. J. Murphy, (2003), Preferential end-to-end assembly of gold nanorods by biotin–streptavidin connectors, *J. Am. Chem. Soc.*, **125**, 13914–13915.

(32) R. Voggu, S. Pal, S. K. Pati, and C. N. R. Rao, (2008), Semiconductor to metal transition in SWNTs caused by interaction with gold and platinum nanoparticles, *J. Phys.: Condens. Matter*, **20**, 215211.

(33) A. Hirsch, and M. Brettreich, (2005), *Fullerenes – Chemistry and Reactions*, Wiley-VCH, Weinheim.

(34) W.-B. Zhang, Y. Tu, R. Ranjan, R. M. Van Horn, S. Leng, J. Wang, M. J. Polce, C. Wesdemiotis, R. P. Quirk, G. R. Newkome, and S. Z. D. Cheng, (2008), 'Clicking' fullerene with polymers: synthesis of [60]fullerene end-capped polystyrene, *Macromolecules*, **41**, 515–517.

(35) J. Iehl, R. Pereira de Freitas, and J.-F. Nierengarten, (2008), Click chemistry with fullerene derivatives, *Tetrahedron Lett.*, **49**, 4063–4066.

(36) J. Iehl, R. Pereira de Freitas, B. Delavaux-Nicot, and J.-F. Nierengarten, (2008), Click chemistry for the efficient preparation of functionalized [60]fullerene hexakis-adducts, *Chem. Commun. (Cambridge)*, 2450–2452.

(37) P. I. Kitov, J. M. Sadowska, G. Mulvey, G. D. Armstrong, H. Ling, N. S. Pannu, R. J. Read, and D. R. Bundle, (2000), Shiga-like toxins are neutralized by tailored multivalent carbohydrate ligands, *Nature*, **403**, 669–672.

(38) H. Isobe, H. Mashima, H. Yorimitsu, and E. Nakamura, (2003), Synthesis of fullerene glycoconjugates through sulfide connection in aqueous media, *Org. Lett.*, **5**, 4461–4463.

(39) H. Isobe, K. Cho, N. Solin, D. B. Werz, P. H. Seeberger, and E. Nakamura, (2007), Synthesis of fullerene glycoconjugates via a copper-catalyzed huisgen cycloaddition reaction, *Org. Lett.*, **9**, 4611–4614.

(40) D. Tasis, N. Tagmatarchis, A. Bianco, and M. Prato, (2006), Chemistry of carbon nanotubes, *Chem. Rev.*, **106**, 1105–1136.

(41) H. Li, F. Cheng, A. M. Duft, and A. Adronov, (2005), Functionalization of single-walled carbon nanotubes with well-defined polystyrene by 'click' coupling, *J. Am. Chem. Soc.*, **127**, 14518–14524.

(42) H. Li, and A. Adronov, (2007), Water-soluble SWCNTs from sulfonation of nanotube-bound polystyrene, *Carbon*, **45**, 984–990.

(43) Z. Guo, L. Liang, J.-J. Liang, Y.-F. Ma, X.-Y. Yang, D.-M. Ren, Y.-S. Chen, and J.-Y. Zheng, (2008), Covalently β-cyclodextrin modified single-walled carbon nanotubes: a novel artificial receptor synthesized by 'click' chemistry, *J. Nanopart. Res.*, **10**, 1077–1083.

(44) S. Campidelli, B. Ballesteros, A. Filoramo, D. Díaz Díaz, G. de la Torre, T. Torres, G. M. A. Rahman, C. Ehli, D. Kiessling, F. Werner, V. Sgobba, D. M. Guldi, C. Cioffi, M. Prato, and J.-P. Bourgoin, (2008), Facile decoration of functionalized single-wall carbon nanotubes with phthalocyanines via 'click chemistry', *J. Am. Chem. Soc.*, **130**, 11503–11509.

(45) J. L. Mynar, T. Yamamoto, A. Kosaka, T. Fukushima, N. Ishii, and T. Aida, (2008), Radially diblock nanotube: site-selective functionalization of a tubularly assembled hexabenzocoronene, *J. Am. Chem. Soc.*, **130**, 1530–1531.

(46) V. P. Torchilin, (2005), Recent advances with liposomes as pharmaceutical carriers, *Nat. Rev. Drug Discov.*, **4**, 145–160.

(47) S. Cavalli, A. R. Tipton, M. Overhand, and A. Kros, (2006), The chemical modification of liposome surfaces via a copper-mediated [3 + 2] azide–alkyne cycloaddition monitored by a colorimetric assay, *Chem. Commun. (Cambridge)*, 3193–3195.

(48) F. Said Hassane, B. Frisch, and F. Schuber, (2006), Targeted liposomes: convenient coupling of ligands to preformed vesicles using 'click chemistry', *Bioconjugate Chem.*, **17**, 849–854.

(49) D. E. Discher, and F. Ahmed, Polymersomes, (2006), *Annu. Rev. Biomed. Eng*, **8**, 323–341.

(50) J. A. Opsteen, R. P. Brinkhuis, R. L. M. Teeuwen, D. W. P. M. Löwik, and J. C. M. v. Hest, (2007), 'Clickable' polymersomes, *Chem. Commun. (Cambridge)*, 3136–3138.

(51) S. F. M. van Dongen, M. Nallani, S. Schoffelen, J. J. L. M. Cornelissen, R. J. M. Nolte, and J. C. M. van Hest, (2008), A block copolymer for functionalisation of polymersome surfaces, *Macromol. Rapid Commun.*, **29**, 321–325.

(52) D. M. Vriezema, P. M. L. Garcia, N. Sancho Oltra, N. S. Hatzakis, S. M. Kuiper, R. J. M. Nolte, A. E. Rowan, and J. C. M. van Hest, (2007), Positional assembly of enzymes in polymersome nanoreactors for cascade reactions, *Angew. Chem., Int. Edn*, **46**, 7378–7382.

(53) B. Li, A. L. Martin, and E. R. Gillies, (2007), Multivalent polymer vesicles via surface functionalization, *Chem. Commun. (Cambridge)*, 5217–5219.

(54) D. M. Vriezema, M. Comellas Aragones, J. A. A. W. Elemans, J. J. L. M. Cornelissen, A. E. Rowan, and R. J. M. Nolte, (2005), Self-assembled nanoreactors, *Chem. Rev.*, **105**, 1445–1490.

(55) R. K. O'Reilly, M. J. Joralemon, K. L. Wooley, and C. J. Hawker, (2005), Functionalization of micelles and shell cross-linked nanoparticles using click chemistry, *Chem. Mater.*, **17**, 5976–5988.

(56) R. K. O'Reilly, M. J. Joralemon, C. J. Hawker, and K. L. Wooley, (2006), Fluorogenic 1,3-dipolar cycloaddition within the hydrophobic core of a shell cross-linked nanoparticle, *Chem. Eur. J.*, **12**, 6776–6786.

(57) M. J. Joralemon, R. K. O'Reilly, C. J. Hawker, and K. L. Wooley, (2005), Shell click-cross-linked (SCC) nanoparticles: a new methodology for synthesis and orthogonal functionalization, *J. Am. Chem. Soc.*, **127**, 16892–16899.

(58) R. K. O'Reilly, M. J. Joralemon, C. J. Hawker, and K. L. Wooley, (2007), Preparation of orthogonally-functionalized core click cross-linked nanoparticles, *New J. Chem.*, **31**, 718–724.

(59) R. K. O'Reilly, M. J. Joralemon, C. J. Hawker, and K. L. Wooley, (2006), Facile syntheses of surface-functionalized micelles and shell cross-linked nanoparticles, *J. Polym. Sci., Part A: Polym. Chem.*, **44**, 5203–5217.

(60) X. Jiang, J. Zhang, Y. Zhou, J. Xu, and S. Liu, (2008), Facile preparation of core-cross-linked micelles from azide-containing thermoresponsive double hydrophilic diblock copolymer via click chemistry, *J. Polym. Sci., Part A: Polym. Chem.*, **46**, 860–871.

(61) Q. Wang, T. R. Chan, R. Hilgraf, V. V. Fokin, K. B. Sharpless, and M. G. Finn, (2003), Bioconjugation by copper(I)-catalyzed azide-alkyne [3 + 2] cycloaddition, *J. Am. Chem. Soc.*, **125**, 3192–3193.

(62) S. Sen Gupta, J. Kuzelka, P. Singh, W. G. Lewis, M. Manchester, and M. G. Finn, (2005), Accelerated bioorthogonal conjugation: a practical method for the ligation of diverse functional molecules to a polyvalent virus scaffold, *Bioconjugate Chem.*, **16**, 1572–1579.

(63) S. Sen Gupta, K. S. Raja, E. Kaltgrad, E. Strable, and M. G. Finn, (2005), Virus–glycopolymer conjugates by copper(I) catalysis of atom transfer radical polymerization and azide–alkyne cycloaddition, *Chem. Commun. (Cambridge)*, 4315–4317.

(64) G. Destito, R. Yeh, C. S. Rae, M. G. Finn, and M. Manchester, (2007), Folic acid-mediated targeting of cowpea mosaic virus particles to tumor cells, *Chem. Biol.*, **14**, 1152–1162.

(65) W.-H. Zhan, H. N. Barnhill, K. Sivakumar, H. Tian, and Q. Wang, (2005), Synthesis of hemicyanine dyes for 'click' bioconjugation, *Tetrahedron Lett.*, **46**, 1691–1695.

(66) E. Kaltgrad, S. Sen Gupta, S. Punna, C. Y. Huang, A. Chang, C.-H. Wong, M. G. Finn, and O. Blixt, (2007), Anti-carbohydrate antibodies elicited by polyvalent display on a viral scaffold, *ChemBioChem*, **8**, 1455–1462.

(67) D. E. Prasuhn, R. M. Yeh, A. Obenaus, M. Manchester, and M. G. Finn, (2007), Viral MRI contrast agents: coordination of Gd by native virions and attachment of Gd complexes by azide–alkyne cycloaddition, *Chem. Commun. (Cambridge)*, 1269–1271.

(68) T. L. Schlick, Z. Ding, E. W. Kovacs, and M. B. Francis, (2005), Dual-surface modification of the tobacco mosaic virus, *J. Am. Chem. Soc.*, **127**, 3718–3723.

(69) M. A. Bruckman, (2008), Surface modification of tobacco mosaic virus with 'click' chemistry, *ChemBioChem*, **9**, 519–523.